In: Troponin
Editor: J.-P. Jin
ISBN: 978-1-62948-320-7
© 2014 Nova Science Publishers, Inc.

No part of this digital document may be reproduced, stored in a retrieval system or transmitted commercially in any form or by any means. The publisher has taken reasonable care in the preparation of this digital document, but makes no expressed or implied warranty of any kind and assumes no responsibility for any errors or omissions. No liability is assumed for incidental or consequential damages in connection with or arising out of information contained herein. This digital document is sold with the clear understanding that the publisher is not engaged in rendering legal, medical or any other professional services.

Chapter V

Conformational States and Behavior of the Heterotrimeric Troponin Complex

Daniel C. Rieck, MSc[1] and Wen-Ji Dong, PhD[1,2*]

[1] Gene and Linda Voiland School of Chemical Engineering and Bioengineering, Washington State University, Pullman, Washington, US

[2] Department of Integrative Physiology and Neuroscience, Washington State University, Pullman, Washington, US

Abstract

Complete understanding of the functions of the heterotrimeric troponin complex rests upon knowledge of its structure. Insights into the physiological structure and conformational behavior of troponin are thus reviewed in this chapter. The primary experimental settings and biophysical methods that have been used to investigate troponin structure are covered first, wherein a critical understanding of the differences between approaches is emphasized. General aspects of the structure and molecular environment of troponin are treated next, starting at the subunit level and ending with a description of how troponin fits into the ultrastructure of the myofilament lattice. Building off of this foundation, the changes in troponin conformational state that lead to its complex regulatory behaviors are then discussed. Overall, it has become clear that the conformational states of troponin and the nature of conversions between them collectively play a central role in determining the physiological contractile behavior of the myocyte sarcomere.

Introduction

The physiological structure and conformational behavior of the heterotrimeric troponin (TN) complex has long been a topic of considerable scientific importance. It is as easy to see

* Correspondence: wdong@vetmed.wsu.edu.

why as the act of seeing itself. Right now, your eyes are moving along this text because of the Ca^{2+}-dependent conformational behavior of TN. TN structure also plays an essential role in maintaining your body posture as you read. When you manipulate the remainder of this text, whether it is in print or digital form, Ca^{2+}-induced changes in the conformational state of TN will enable you to turn your thoughts into muscular action. While reading, your heart will faithfully and involuntarily pump blood throughout your body thanks also to Ca^{2+}-dependent structural changes in TN. The Ca^{2+} responsiveness of TN conformational state not only provides these types of control over muscular force generation in *Homo sapiens*, but also in an evolutionary panoply of vertebrates and invertebrates. It is this impressive biological milieu in which the science of TN structure finds both its context and aim.

This science has advanced considerably in recent decades as the conformational behavior of TN has been increasingly illuminated by numerous lines of investigation. The field necessarily started with studying TN and its subunits in relative biochemical isolation. Invaluably detailed crystal structure models of the TN core domain have emerged from X-ray diffraction (XRD) studies on *H. sapiens* cardiac TN (cTNC) [1] and *Gallus gallus* fast skeletal TN (sTN) [2]. As important as this structural information is, our field has built substantially on the relatively static, artificial, and isolated picture of TN given by X-ray crystallography. Through a variety of other techniques, the dynamic and contextual nature of the relationship between TN conformation and function has progressively come to light under increasing levels of physiological approximation. Methods for studying TN structure *in situ* have even been developed. Overall, it is now much clearer how the Ca^{2+}-dependent conformational behavior of TN is intricately complex, intensely allosteric, isoform specific, and continually modulated by the presence and activity of other proteins found in the sarcomere.

To explore the structural behavior of TN is to immerse oneself in the mystery and wonder of what protein chemistry achieves in muscle. The primary goal of this chapter is to fortify within the reader a critical familiarity with what has been learned about TN structure and its functional role in muscle physiology. An important secondary goal is to help the reader grasp the key scientific problems that remain in the field of TN structural study. The chapter is broadly structured to first review the basics of TN structure from a cellular physiology perspective and then discuss the conformational behavior of TNin detail while focusing on the more advanced developments of our field that have been made in the last decade. Accordingly, after introducing the complexities inherent in the study of TN conformational behavior, we will begin with a critical overview of the key experimental methods that have been employed. Next, we will explore the structure of TN starting at the subunit level and proceeding to its arrangement in the architecture of the sarcomeric thin filament (TF). This will serve as a foundation for discussing the effects of Ca^{2+}binding and dissociation and strong cross-bridge (sXB) formation on the conformational state of TN. We will thus conclude with a mechanistic treatment of how these changes in TN conformation serve as the structural basis for the ability of TN to regulate sarcomeric force generation.

The Importance of Conformational State to Troponin Function

The concept that a protein's structure dictates its function is the axiomatic premise behind the quintessential hypothesis of structural biology investigation. When engrossing oneself in the study of TN structure, it is therefore important to remain cognizant of the physiological

context and evolutionary purpose of TN. TN serves a regulatory role in the TFs found in the highly organized and force-generating myocyte sarcomere, one of Nature's most complex macromolecular assemblies [3]. Accordingly, the *prima facie* identity of TN is that ofa complex of binding proteins. TN binds divalent cations like Ca^{2+} and other TF proteins such as actin and tropomyosin, but seems to perform no other discernible chemistry. It is only after the structural behavior of TN is closely examined that the subtlety of its characteristics becomes more evident. Though TN is not strictly an enzyme, the Michaelis Menten model nevertheless accurately describes the kinetics of Ca^{2+}-induced TN conformational changes[4]. This suggests that TN serves as both "catalyst" and "substrate" for producing reversible changes in its own structure. The useful "product" that TN affords the myocyte is the Ca^{2+} dependent conversion between its conformations because those conformations either inhibit or promote sarcomeric force generation. The integrity of not only the conformational conversion process but also the conformations themselves is therefore physiologically significant [5]. Therein lays the importance of studying TN structure.

The conformational conversion function of TN has been referred to in the past as Ca^{2+}-regulated switching (CRS) [6,7] and TN itself has been called a Ca^{2+}-sensitive molecular switch [8]. The mechanism underlying CRS is deceptively simple. TN possesses Ca^{2+} sensing functionality akin to calmodulin (CaM) such that its conformation changes in response to Ca^{2+} binding or dissociation. ItsCa^{2+}-dependent structural changes have evolved to function as a binary switch in turning sarcomeric force generation "on" or "off." Thus CRS represents a highly specialized form of second messenger regulation that has been integrated into the sarcomeric thin filament (TF). TN transduces second messenger Ca^{2+} signals into TF protein conformational changes and thereby provides the regulatory signaling mechanism necessary for controlling muscular force. Though some details of the mechanism involved are isoform specific, the binary switching concept of TN function appears universal [9]. Nevertheless, the more that has been learned about the conformations of TN and how they change, the clearer it has become that CRS is far more complex than a simple matter of "on or off."

CRS involves ensemble behavior, energetic balance, dynamics, and kinetics. Ca^{2+}-triggered conformational changes in TN and other TF regulatory proteins take time, and it also takes time for the actomyosin cross-bridge cycle to respond accordingly. This adds a layer of additional complexity to TN structural study that is compounded by the significant differences between the *in vivo* molecular environment and what is present during experimentation. Thus, the physiological kinetics of CRS are still largely unknown, as are any changes to normal kinetics that are caused by mutations and post translational modifications (PTMs). There are many other fundamental uncertainties surrounding the structural mechanism underlying *in vivo* CRS that need to be addressed. Particularly, the structural basis for the role of TN in effecting the cooperativity and sarcomere length dependence of Ca^{2+}-dependent TF activation remains largely uncharacterized. Hence, in spite of years of considerable progress made in the study of TN structure, there remains much to learn through additional scientific inquiry about the physiological conformational behavior of TN.

Methods for Studying Troponin Structure

The scientific goal of our field is to gain a complete understanding of the how *the in vivo* conformational behavior of TN relates to its physiological function. We aim to evolve this understanding from accumulating experimental observations made under a particular setting using some combination of methods. Every overall approach has both benefits and drawbacks, and it is vital to be cognizant of such pros and cons. A brief critical survey of the settings and methods that have been used in structural studies of TN reveals the difficulty of our goal: the elucidation of the physiological relationship between TN structure and function.

Experimental Settings

In the context of this review, "setting" represents which isoform of TN is being studied and what kind of molecular environment is being used in an experiment. Each type of environment aims to achieve some form of balance between interpretational simplicity and reproduction of native complexity. One must nevertheless recognize that protein folding and binding are inexorably a function of molecular environment. It is not only the primary sequence of TN subunits that will dictate their stable conformations and binding affinities. Other important determinants include solvent properties and the influence of the other biomolecules present in the sarcomere. Keeping that caveat in mind, the three settings wherein significant advances have been made in our knowledge of TN structure are *in vitro*, *in situ*, and *in silico*.

The In Vitro Setting

TN structural study began *in vitro* and enjoys a long and fruitful history with this setting. Typically, recombinant isoforms of one or more TN subunits are first bacterially expressed and purified. They are combined with each other and other purified sarcomeric proteins if desired. They are then structurally characterized under some biochemical condition. The major advantages of *in vitro* investigation are isolation and controlled integration. A TN subunit may first be studied alone, next when integrated into the whole complex, and finally when integrated into reconstituted TFs. This allows for the relatively unambiguous interpretation of changes in structural behavior and the potential determinants of physiological conformational behavior can thus be identified more easily. Higher resolution structural methods such as XRD and nuclear magnetic resonance (NMR) are still almost solely compatible with the *in vitro* experimental format due to its simpler preparations.

The major disadvantage of the *in vitro* setting is that the level of physiological approximation is very slight even under the best case. The most physiologically representative *in vitro* setting has been the reconstituted TF, wherein whole TN is integrated into F-actin along with TM. Additionally, myosin subfragment-1 (S1) may be added to simulate the presence of XBs. However, a familiarity with the field of sarcomerogenesis makes one realize just how different reconstituted TFs are from what occurs naturally in myocytes [3, 10]. Molecular rulers are missing *in vitro*, structural and elastic elements are not present, and components are "assembled" *via* unguided binding equilibria. Force cannot be generated and sarcomere length dependence cannot be studied because the sarcomere lattice

is absent. Since the cooperativity of Ca^{2+}-dependent TF activation is greatly attenuated *in vitro* relative to *in situ*, significant allosteric pathways for modulating TN conformational state must also be missing. Nevertheless, the *in vitro* setting has produced many useful insights into TN conformational states and the Ca^{2+} and XB dependent conversions between them.

The In Situ Setting

Our field has recently developed abilities to investigate TN structure when found in the relatively intact sarcomeres of isolated muscle tissue. Though the *in situ* setting is not technically *in vivo*, it has allowed structural investigation to begin approaching the physiological environments in which TN is naturally found. Generally, tissue is dissected from a particular organism and chemically skinned to remove myocyte membranes and their associated proteins. Demembranation allows direct access to sarcomeric proteins and experimental control over the solution that bathes myofilaments. Also, TN constructs with any mutations and fluorescent labels may be verifiably swapped with endogenous counterparts. The stability of chemically skinned *in situ* preparations is fortunately quite good even at room temperature when reducing agents and protease inhibitors are present [11]. Thus, the advantage of the *in situ* environment is that the experimentalist works with preparations that are the product of actual sarcomerogenesis. Components absent *in vitro* are now present, and one can investigate how TN conformational behavior relates to force generation, sarcomere length, and a more realistic level of cooperativity.

The disadvantage of the *in situ* setting is that control over experimental variables comes at a compromise. Demembranation changes sarcomere lattice spacing [12], and skinned fibers have poor stability at physiological temperatures such that room temperature *in situ* studies are preferred[13]. Muscles can come from many different organisms, leaving one to wonder about their *in vivo* differences and consequent interpretational subtleties. Most *in situ* structural techniques to date have been based on fluorescence spectroscopy and therefore require that endogenous TN subunits are substituted with fluorescently labeled recombinant preparations. Labeling often requires site directed mutagenesis in addition to the covalent addition of bulky fluorophores to protein structure. However, since protein structures frequently mutate during evolution with little functional consequence, there is good reason to take seriously the data from labeled TN constructs that have been carefully experimentally controlled. In spite of its limitations, the *in situ* setting is much closer to *in vivo* than *in vitro* alternatives and can add much new information to the science of TN structure.

The In Silico Setting

It may seem that use of the *in silico* setting is moving even further away from the physiological environment of TN than the *in vitro* setting. Nevertheless, computational simulation has an important and useful place in the study of TN structure. The principal approach used *in silico* is the Monte Carlo method. Simulation proceeds from a solvated starting structure of the proteins under investigation. As simulated time passes, the protein is allowed to stochastically search through its conformational space according to the same thermodynamic constraints that determine real world conformational behavior. Thus the major advantage of the *in silico* setting is that it can provide powerful answers about the likelihood of conformational possibilities that cannot readily be studied. It is useful for determining how TN mutation likely changes intra-protein residue contacts known from XRD

or NMR, or the probable behavior of TN regions too dynamic to be confidently resolved from XRD data.

The obvious disadvantage of *in silico* methods is that modeling the reality of protein chemistry is computationally intensive and fundamentally challenging. This is why the virtual environment of probabilistic, stochastic simulation, the quintessential *in silico* approach, resembles the *in vitro* rather than the *in situ* setting. Another consequence of computational limitations is that conformational behavior may currently be simulated up to nanosecond time scales at most. Many physiologically important events that occur on slower millisecond time scales cannot yet be simulated. Finally, *in silico* methods are geared toward equilibrium and finding the stable conformations of a molecule. Important but short lived intermediates that may be involved in conversions between conformations will likely be missed. Though one should be careful when interpreting *in silico* predictions for these reasons, the probabilistic information provided about TN structure is still very useful.

Structural Measurement Techniques

Quantum physics is the fundamental science that makes the biophysical measurement of TN structure possible. Even a basic understanding of molecules as quantum systems can prove illuminating when thinking critically about TN structural studies. Like any molecule, TN is an entity with a dynamic structure wherein spinning electrons in constant motion are localized to spinning nuclei in a manner describable by a three dimensional wave function. This behavior stems from how underlying fundamental forces driven by charges are kept in a continual balance. Electron orbitals may be thought of accordingly as energetically optimized "clouds" of dynamic nuclear localization. If an electron were localized any more "tightly" than the cloud it is stably occupying, its electric potential energy would decrease less than its kinetic energy would increase; hence the balance achieved by the orbital. Of course, the dynamic balance of forces in a molecule may be changed to a higher energy state if the right amount of energy is somehow supplied. All structural techniques depend on observing how the balance of forces in a molecule interacts with some form of externally applied force.

Fluorescence Spectroscopy

Many studies of TN structure have relied on fluorescence spectroscopy, wherein one observes the complex interaction between an externally applied electromagnetic force and a fluorescent molecule [14]. Photons are energy in the form of a harmonically oscillating electromagnetic field propagated through space. If an incident photon is oscillating at a certain frequency, it can supply the exact amount of applied electromagnetic force needed to change the localization of a valence electron within a fluorophore. Within femtoseconds, photonic energy will "excite" the electron away from its ground state orbital to occupy an orbital of higher electric potential energy. The distribution of Coulombic charge within the fluorophore, represented by a dipole moment, consequently changes. Excitation can also cause the fluorophore to vibrate more energetically. Accordingly, it is common for a photon absorbing fluorophore to become both vibrationally and electronically, or vibronically, excited. Compared to the energy required to change a fluorophore's vibrational mode, the energy required to change valence electron localization is two orders of magnitude greater. Thus, many vibrational modes might be accessible from the supplied excitation energy.

The lowest energy excited state is only semi-stable such that fluorophores typically exhibit ~10 nanosecond fluorescence lifetimes. An excited fluorophore will spontaneously relax to its ground state through one of several possible pathways. Emission occurs when the excited electron spontaneously returns to its ground state orbital and in the process emits self-propagating electromagnetic waves. Relaxation can also occur non-radiatively through external conversion wherein electronic excitation energy is dissipated through collision with neighboring solvent molecules. Collisional quenching is similar but involves solute instead of solvent molecules. A fluorophore can even resonantly transfer its excitation energy to a neighboring fluorophore if certain conditions are met. Ultimately, the quantum yield, or probability that emission will be the electronic relaxation pathway that follows an excitation event, depends both on a fluorophore's structure and the nature of its molecular environment.

Though the energy of an emitted photon can be equal to that of the exciting photon, it is generally less. This happens because some of the exciting photon's absorbed energy can be lost in several ways prior to emission. For instance, through picosecond internal conversion an excited electron will non-radiatively relax to an orbital at one electronic energy level above the ground state regardless of how many energy levels it initially gained. Similarly, a vibrationally excited fluorophore will thermally transfer its excess vibrational energy to its environment within picoseconds. Some energy may also be lost when surrounding solvent dipoles are induced into alignment with the excited state dipole of the fluorophore. Additionally, though emission returns the excited electron back to its ground electronic energy level, it can leave the fluorophore in one of generally many possible excited vibrational modes. These types of energy losses are responsible for the Stokes shift, or energetic difference between excitation and emission maxima, that makes fluorophores so useful as a molecular label.

Environmentally Sensitive Fluorescent Probes

The high sensitivity of some fluorophores to environmental conditions can be employed for structural investigation. A conversion between a protein's conformational states can involve changes in the polarity of the local environment at certain locations within the protein. When a fluorophore is attached to such locations, its maximal emission intensity will change as a function of conformational state if its quantum yield is significantly affected by polarity. This is the idea behind using environmentally sensitive fluorophores as an indicator of TN structural transitions. The method is well suited to TN structural study because CRS involves the binding of positively charged Ca^{2+} and changes in the solvent exposure of hydrophobic regions within TN [15]. Environmentally sensitive fluorophores have been used extensively to study the binding of Ca^{2+} to TN *in vitro* and have recently also been employed *in situ* [16, 17]. One major advantage of environmentally sensitive fluorophores is that they can be used to measure the kinetics of changes in local polarity associated with changes in TN structure. The main disadvantage of the method is that it provides little structural detail other than indicating that a conformational change has occurred. Furthermore, if a TN structural transition occurs without producing a change in the polarity of the probe's local environment, the transition will not be detected [18].

Fluorescence Anisotropy

The experimentalist can use anisotropy to exploit the polarized nature of fluorescence in measuring regional protein flexibility and orientation [14]. Photons are absorbed and radiated

by a fluorophore along its excitation and emission transition dipole moments, respectively. If vertically polarized excitation light is focused on a fluorescently labeled sample, those fluorophores whose excitation transition dipole moments happen to be vertically aligned will be preferentially excited. The orientation of these selectively excited fluorophores will then begin to randomize due to rotational diffusion associated with stochastic molecular motion. The vertically and horizontally polarized emission intensity from the sample can thus be measured to determine the extent of rotational diffusion that occurs over the duration of the excited state. The more the vertical and horizontal emission intensities overlap, the more the orientations of the selectively excited fluorophore population must have randomized from rotational diffusion. Hence, anisotropy gives information about the inertial susceptibility of labeled species to thermal forces.

Anisotropy can be measured under both steady-state and time-resolved conditions. When time-dependent anisotropy measurements are conducted, fluorescence anisotropy will decay with time according to the kinetics of the underlying rotational diffusion processes that contribute to changes in excited probe orientation. Processes for TN can include the stochastic motions of the thin filament, the core domain, regional subunit structure, and the fluorophore itself [19]. Fluorophore tumbling is generally much faster than the fluorescence lifetime, whereas thin filament and core domain motions are practically negligible due to the large molecular sizes involved. Regional protein structural motions occur on the order of the fluorescence lifetime. Anisotropy can therefore provide information about regional protein dynamics [19] and spatial orientations [20].

The main advantage of anisotropy is its ability to provide information about protein dynamics in very large molecules such as TN when integrated into the thin filament. It has worked not only *in vitro* [19], but also in *situ*. Two bifunctional rhodamines can been attached to an α-helix in TN and crosslinked. A fiber containing labeled TN can then be illuminated with excitation light aligned either in parallel with or perpendicular to the fiber axis [20-22]. This provides a quantitative measure of changes in regional α-helical orientation [21] or even TN core domain orientation [20] during CRS. The main disadvantage of anisotropy is that time window for observation of rotational diffusion is limited to the fluorescence lifetime of the probe. Also, like any fluorescence technique, anisotropy requires careful fluorescence labeling that may even involve site directed mutagenesis to generate single or double cysteine mutants amenable to the desired placement of probes.

Förster Resonance Energy Transfer

Förster resonance energy transfer (FRET) is a powerful and versatile structural technique often described as a spectroscopic ruler [14]. To understand how FRET works, note that an excited fluorophore can be accurately described as an oscillating dipole, which is analogous to a tuning fork. Accordingly, every fluorophore has a resonant frequency. If exposed to an electromagnetic field oscillating at that frequency, a fluorophore will convert the energy of that field into its own oscillation. Oscillating dipoles generate "near" and "far" field components. The near field is dominated by the strength of the dipole's own electromagnetic field that, which has time variant electric and magnetic field components. Since time variant electric fields generate magnetic fields and *vice versa*, dipole oscillation produces secondary radiative field components whose strength dominates the far field. The dipole and radiative field strengths decay according to inverse cube and square power laws, respectively. FRET takes place within the near field, where absorption of electromagnetic field energy by the

acceptor causes the excited state donor dipole to cease oscillating. Thus the excited donor valance electron becomes relaxed while the acceptor valance electron becomes excited.

FRET can occur between a donor and an accepter fluorophore pair where the donor emission spectrum overlaps with the acceptor excitation spectrum. This translates to overlap between the energetics of the vibronic emission and excitation transitions of the donor and acceptor, respectively. Another requirement is that the transition dipole moments of the donor and acceptor are parallel. If these conditions are met, then FRET will occur with an efficiency governed by an inverse 6^{th} power law and involving a unique Förster critical distance commonly denoted R_0. Note that R_0 depends on the orientational freedom of the fluorophores. When the donor and acceptor are spaced apart by R_0, FRET is 50% efficient. FRET efficiency can be determined by measuring donor and acceptor fluorescence intensities or lifetimes, the latter of which is preferred because it is independent of fluorophore concentration.

Depending on the pair of fluorophores chosen by the experimentalist, FRET is useful for measuring molecular distances ranging from approximately 10 to 100 Å. FRET is fortuitously independent of molecular environment. Other advantages of FRET are its high sensitivity to alterations in inter-probe distance, suitability for measuring a range of distances significant to protein conformational changes, compatibility with the *in situ* setting, and ability to measure the kinetics of changes in molecular distance. Multi-acceptor FRET can even be used to determine the orientation of TN in the TF, but the experiment involved is complex and challenging to interpret correctly [23]. Its two main disadvantages are that it requires labeling with multiple fluorophores, and that R_0 must be determined indirectly in a manner that includes assumptions about relative dipole orientations and freedom of movement. Furthermore, FRET measurements must be carefully controlled. Measurements of the donor emission in the absence of acceptors are a must, and conformational changes must not end up limiting the freedom of probe orientation.

Protein Crystallization and X-Ray Diffraction

XRD is another structural technique wherein the interaction between electrons and electromagnetic radiation is observed [24]. Compared to fluorescence, one works with higher energy X-ray photons that are 0.5–2.5 Å in wavelength; and instead of depending on the excitatory absorption of photons by electrons, XRD instead relies on electrons to scatter photons. Scattering is caused by electromagnetic field oscillations associated with an incident X-ray as it is propagated into matter. Electrons are acted upon by the electromagnetic field to oscillate at the same frequency as the X-ray, and the associated charge motions induce a secondary electromagnetic field oscillation also of the same frequency. This secondary electromagnetic field oscillation is propagated in all directions. If scattering occurs from an array of atoms that are appropriately spaced and basically immobile, the X-ray waves produced by that scattering can undergo interference to produce diffracted rays arranged in a pattern representative of underlying atomic structure. Crystal lattices contain the ordered and immobilized atomic arrays needed to diffract X-rays in this manner.

Crystallization is the process whereby a folded protein is converted from its dynamic state in solution into repeating units of ordered and immobilized atomic arrangement suitable for XRD. Protein crystallization is still something of an art form but generally involves the achievement of a supersaturated protein-precipitant solution, prepared from highly purified protein, whose conditions are ideal for the stability and crystallization of the protein of interest [25]. The crystals produced are principally held together by hydrogen bonding

between hydrated protein surfaces and must be of adequate size for handling. If a crystal can obtained and imaged, then its XRD patterns can be interpreted into an electron density map. Since atoms of greater electron density will produce diffracted rays of greater intensity, XRD gives information about atomic position and identity.

The advantage of a good XRD study is the detailed Å resolution structural information it provides. Because crystals are formed from folded proteins, it is reasonable to expect that crystal structures will be representative of *in vivo* conformational states. Though XRD is an incredibly useful structural tool, it does have several disadvantages. Because a crystal lattice is required to produce interpretable XRD patterns, TN must first be rendered into crystalline form. This makes high resolution XRD visualization of TN when incorporated into the reconstituted TF impossible, much less an *in situ* XRD study of Å level resolution. Another issue is when TN constructs have successfully been crystallized in the past, their numerous dynamic regions have stayed disordered and proved unresolvable [1,2]. Finally, the conformational state that TN adopts in a crystal may differ from *in vivo* wherein the molecular environment is different and all binding partners are present. This is an important caveat applicable to any high resolution XRD study.

Nuclear Magnetic Resonance

Whereas fluorescence spectroscopy and XRD are focused primarily on electrons, NMR spectroscopy is concerned with an interaction that can occur between certain atomic nuclei and radio frequency electromagnetic radiation [26]. When nuclei possessing net magnetic spin are immersed in a static magnetic field, their magnetic moment will spontaneously align with the external field. The amount of applied electromagnetic force required to invert the moment against the external field is within the range of energy stored in radio frequency photons. The frequency of incident photon required to invert the spin of a particular nucleus depends on the effective strength of the external field felt by the nucleus and a gyromagnetic ratio that is determined by nuclear structure. The effective field strength is generally less than the external field strength because the electrons localized to the nucleus will create secondary magnetic fields that generally oppose the external field. Because electron localization depends on the type of nuclei and bonds present in a molecule, photon absorbance indicates not only the presence of particular nuclei but also the nature of their local chemical environment.

The selective spin inversion concept underlying NMR can be cleverly exploited to gain a wealth of structural information and makes NMR an amazingly versatile tool for structural study. NMR experiments can characterize the energetic coupling between spin nuclei mediated through covalent bonding and thereby map out molecular connectivity and associated bond distances and angles. Measurement of the nuclear Overhauser effect can provide inter-nuclear distances between localized nuclei that are not connected by bonding. By performing multidomain heteronuclear measurements on the resonant frequencies of multiple types of spin nuclei (e.g. ^{1}H, ^{13}C, ^{15}N), three dimensional structures of entire proteins can be resolved from NMR data. Heteronuclear experiments do require that isotopically substituted recombinant constructs of the protein of interest are generated. Finally, NMR can be conducted in a time resolved format to obtain information about the dynamics and kinetics of protein conformational changes.

The major advantages of NMR are its versatility and ability to provide dynamic structural information of atomic resolution about protein structure in solution. Unfortunately, for the time being NMR is effectively an *in vitro* technique as far as high resolution is concerned.

Resonance congestion becomes problematic at large molecular sizes, and conventional multidimensional heteronuclear NMR spectroscopy is limited to ~35 kDa proteins. Even whole fast skeletal TN from *H. sapiens* is 70.1 kDa and is therefore too large, so past NMR studies have been on TN subunits either in isolation or in the presence of peptidic reductions of binding partners. The recent development of protein deuteration techniques to reduce the complicating spin inversion relaxation pathways associated with ^{1}H has allowed NMR to be useful for studying ~100 kDa sized proteins [27]. Nevertheless, just one *H. sapiens* cardiac TF structural regulatory unit (sRU) is a staggering ~731 kDa. It may be possible to study isotopically substituted recombinant TN subunits in cultured myocytes, but a truly *in situ* high resolution NMR experiment is currently beyond the reach of the technique. However, molecular-scale magnetic resonance imaging may one day be possible [28].

Electron Paramagnetic Resonance

Electron paramagnetic resonance (EPR) is a powerful technique that is very similar to NMR, but like FRET it can be used to measure long range atomic distances [29]. EPR involves the energetics of inverting electron spin in an externally applied magnetic field. This typically requires that a protein is labeled with a probe containing an unpaired electron whose spin can be freely manipulated by electromagnetic field changes. Electron spin inversion is triggered by microwave photons under the typical approach. As in NMR, spin inversion is energetically coupled to the molecular environment of the spin label. Spins that are sufficiently localized near each other can become energetically coupled through a long-range dipole–dipole interaction, analogous to the concept that underlies FRET. Pulsed electron-electron double resonance (PELDOR) is the experimental approach that takes advantage of this phenomenon and it can be used to measure atomic distances over 8 nm in length.

The advantage of PELDOR over FRET is that spin labels are much smaller and less structurally perturbing than fluorophores. Furthermore, the same spin label is attached to both locations of interest in the protein, whereas FRET requires a more complex labeling scheme involving distinct donor and an acceptor fluorophores. Finally, PELDOR distances are determined directly and therefore do not depend on the uncertain orientation parameter required for converting FRET efficiency to molecular distance. However, FRET is technically more sensitive on a per-probe basis and can be conducted *in situ* and at more physiological temperatures. The advantage of general EPR methods is the incredible specificity of spin labeling because the native electrons found in proteins and typical solvents are generally paired. Much less sample is consequently needed for EPR than NMR or XRD and molecular size is no longer a problem; EPR has been used to study TN *in situ*[30], as has PELDOR [31]. The disadvantages of EPR are otherwise the same as NMR, except that spin labeling is required in EPR whereas in NMR it is not.

Electron Microscopy, Hydrogen/Deuterium Exchange and Other Methods

A variety of other structural measurement techniques have proven very useful in the study of TN structure. Low dose transmission electron microscopy (EM) can visualize the structure and orientation of TN on reconstituted thin filaments *in vitro* [32]. EM takes advantage of the wave-particle duality of electrons to image specimens with subnanometer resolution using a magnetically and electrostatically manipulated electron beam. The Compton wavelength of an electron is ~2.42 pm, which is $>10^{5}$ times shorter than highest energy visible light. Amide hydrogen/deuterium (H/D) exchange can be combined with mass

spectrometry in what represents a powerful and sensitive new approach for determining Ca^{2+}-dependent changes in regional TN dynamics and solvent exposure [33]. Small angle neutron scattering can be used to probe the size and shape of TN [34]. Circular dichroismis another fluorescence spectroscopy technique, and it can be used to determine protein secondary structure because chiral excitation light interacts uniquely with α-helical chirality [35]. Linear dichroism can measure the degree of ordered orientation in TN regional structure with respect to the thin filament axis [36]. Single molecule methods have the potential to identify subpopulations of conformational states normally obscured by ensemble averaging [37]. Finally, biochemical methods can identify structural regions within TN and clarify their functional importance and interaction sites, paving the way for further biophysical investigation [38].

Many useful techniques are clearly available to the experimentalist interested in studying TN structure. However, if one thing can be learned from the above review of the methods used in TN conformational studies, it's that no technique is without its drawbacks. Every technique also has its strong points and these strengths are often unique. Overall, the field of TN structural study is thus at its best when a variety of techniques are being employed and structural information is steadily accumulating from numerous lines of investigation. As will be demonstrated below, it is this kind of multifaceted investigative environment that has led to our field's recent advancements in a contextual understanding of TN structure.

The Structure and Conformational Environment of Troponin

The physiological conformational behavior of TN finds its context in the ultrastructure of the sarcomeres found in striated muscle. To properly interpret TN structural information, it is therefore essential to have at least a basic awareness of the complex structural arrangement of proteins from which the sarcomere is built. This section will review what is known about how TN fits into sarcomeric ultrastructure. The most straightforward way to work with TN has been when it is out of context, and the field of TN structural study began in this manner. However, as our science has progressed, TN conformational behavior has progressively been investigated at increasing levels of physiological approximation. This section will begin accordingly by concentrating on the structural details of each subunit within the TN complex. The view will then broaden to inspect how TN subunits are combined and integrated together into the architecture of the TF. Finally, the ultra structural relationship between the TF and other sarcomeric components, the thick filament especially, will then be discussed. The information reviewed in this section is not only from TN structural studies [8, 39] of interest here but also a considerable history of biochemical investigation [40, 41].

Subunit Level Structure

Regardless of isoform or tissue type, the physiological TN complex is assembled from three subunits: troponin C (TNC), troponin I (TNI), and troponin T (TNT). The letters in this terse naming scheme hint at what is traditionally perceived to be the primary function of each subunit. TNC is the ~18 kDa Ca^{2+} sensor of the TN complex that is ultimately required for

transducing second messenger Ca^{2+} signals into regulatory conformational changes. TnI is a ~24 kDa extended binding protein that inhibits actomyosin ATPase activity, and thereby grants Tn its regulatory power over muscular force generation. TnT is a larger 30-35 kDa extended binding protein that not only binds to TnC and TnI, but also binds strongly to tropomyosin to play a scaffolding role in anchoring the Tn complex to the thin filament. However, structural information has emerged that suggests that TnC, TnI, and TnT are much more than a Ca^{2+} sensor, inhibitor and anchor, respectively. It is now known that each of these subunits plays a complex, modulatable role in the physiological changes in Tn conformation that underlie Tf regulation of muscle contraction.

Troponin C

TnC is the most evolutionarily conserved subunit of Tn. Its structure closely resembles that of CaM [42], the Ca^{2+} binding messenger protein ubiquitously found in eukaryotes [43], and may be crudely described as "dumbbell shaped." Like CaM, it possesses two globular domains (e.g., *H.sapiens* $cTnC_{1–81}$ and $cTnC_{96–161}$) tethered to one another through a central flexible linker (e.g., *H. sapiens* $cTnC_{82–95}$). Both the N- and C-domains of TnC consist primarily of two Ca^{2+}-binding EF-hand motifs. Each EF-hand is essentially a helix-turn-helix motif consisting of two α-helices linked by a 12 residue Ca^{2+}chelation loop. This makes for a total of eight EF-hand α-helices (sequentially labeled A-H from N- to C-terminus) and four potential EF-hand Ca^{2+}-binding sites (labeled I-IV) within every TnC isoform. The chelating ability of TnC E-F hand loops stems from electronegative residues positioned ideally for coordinating cations in a pentagonal-bipyramidal geometry [44]. The α-helices of each TnC E-F hand motif are amphiphilic, containing both polar and nonpolar residues. This allows both the N- and C-domains of TnC to achieve their globular fold which exhibits a buried hydrophobic core and polar solvent exposed surface. Thus the ligand free form of TnC bears a striking resemblance to ligand free CaM.

Unsurprisingly, the Ca^{2+}-saturated conformation of TnC is also very similar to that of CaM. When Ca^{2+} binds to an active TnC Ca^{2+}-binding site, the E-F hand motif reorients itself around Ca^{2+} to facilitate cation coordination [45]. Generally, when Ca^{2+} ions are bound to both binding loops within a TnC globular domain, the reorientation of that domain's E-F hands "opens" the domain and reorganizes its hydrophobic core into a solvent-exposed patch. As is the case with CaM, the exposed hydrophobic patch represents a previously concealed surface for protein–protein interaction that can bind an amphiphilic α-helix which bears complimentary hydrophobic regions. This functionality allows TnC to be integrated into the Tn core domain and interact with TnI as part of CRS. Also, it is the change in polarity that accompanies Ca^{2+} binding and hydrophobic patch exposure that has made environmentally sensitive fluorophores such successful indicators of changes in TnC conformational state.

The structure of each globular domain andTnCCa^{2+}-binding site is tuned by evolution to either achieve a particular Ca^{2+}-binding affinity and specificity or even deactivate divalent cation binding altogether [46]. Site activity is very important for Ca^{2+}-induced domain opening. It is determined by the integrity of the Ca^{2+}-chelation loop and its highly conserved coordinating residues [47]. Site affinity and specificity depend on the primary sequences of the Ca^{2+}-chelation loop [48], its flanking helices [47], and other nearby helices [49]. Affinity is also influenced by interaction between neighboring loops within a domain [50]. Sites III and IV in the C-domain of TnC (C-TnC) have a relatively high affinities for Ca^{2+} ($K_d \approx 10^{-7}$

M) and Mg^{2+} ($K_d \approx 10^{-3}$ M) if active [35]. Sites I and II of the N-domain of TnC (N-TnC) have a lower Ca^{2+} affinity ($K_d \approx 10^{-5.3}$ M), but bind Ca^{2+} with high specificity.

Structural diversity in TnC especially concerns Ca^{2+}-binding site activity. Sites II-IV are active throughout vertebrate striated muscle TnC isoforms. Site I is active in sTnC, but disabled in cTnC due to chelation loop mutations [35]. This structural difference is a contributor to the unique conformational behaviors of N-cTnC and N-sTnC that are important for achieving tissue-specific CRS mechanisms. Particularly, Ca^{2+}binding to N-cTnC is essential but by itself inadequate for completely exposing the hydrophobic patch [51-54]. Invertebrate muscle contains additional TnC variants in indirect flight muscle (IFM) with surprising differences from vertebrate homologues [9]. Sites I-III are disabled in F1-TnC and the remaining site IV binds Ca^{2+} with K_d = 0.16 µM. F1-TnC thus lacks regulatory Ca^{2+}-sensing ability. Furthermore, unlike vertebrate TnC, Ca^{2+}binding to F1-TnC site IV will completely expose the C-domain hydrophobic patch [55]. In F2-TnC, sites I and III are disabled, and the Ca^{2+} affinities of sites II and IV are described by K_d = 180 and 2.6 µM, respectively. The apparent evolutionary purpose behind CRS in IFM is correspondingly different in IFM. Force generation is regulated by Ca^{2+} and modulated by sarcomere length in vertebrate muscle, whereas it is regulated by both Ca^{2+} and sarcomere length in IFM [56].

Owing to its high Ca^{2+}sensitivity, it is commonly found that divalent cations are constitutively bound to the active Ca^{2+} binding sites of C-TnC *in vivo*[44]. The C-domain hydrophobic core is accordingly constitutively exposed, affording to C-TnC a scaffolding role wherein it spontaneously integrates itself with the regions of the other Tn subunits that form the core domain [57]. In contrast, the low Ca^{2+}sensitivity of active Ca^{2+}-binding sites of N-TnC ensures that they are ligand free at basal Ca^{2+} levels. In addition, the Ca^{2+}-binding affinity of these sites is also tuned such that physiological increases in Ca^{2+} will result in the binding of Ca^{2+} that is necessary for complete opening of N-TnC and concomitant exposure of the hydrophobic patch. As will be explained further, N-TnC hydrophobic patch interacts with the C-terminus of TnI (C-TnI) as part of CRS. Thus N-TnC exhibits the regulatory conformational behavior that would be expected for a CaM-like protein that has evolved to be the sarcomere's directly-integrated, dedicated Ca^{2+}-sensor.

Troponin I

TnI is the subunit whose switchable protein–protein interactions are key to the regulatory power of Tn. TnI exhibits an elongated structure [58] possessing the conformational plasticity required for TnI to exchange its binding partners as part of CRS [8]. Six consecutive regions within an N-domain and a C-domain may be identified within vertebrate TnI according to their diverse functions. Starting from the N-terminus, the structure of the N-domain of TnI(N-TnI) begins with a 30 residue cardiac specific region termed the N-terminal extension (N-Ext)[8]. N-Ext-cTnI contains PKA-mediated phosphorylation sites at Ser-22 and Ser-23 (i.e., residue locations in the *H. sapiens* isoform) and may be subdivided into an acidic N-terminus ($cTnI_{1–10}$), a rigid linker ($cTnI_{11–19}$), and a C-terminal α-helix [59].The N-Ext-cTnI is followed by a C-TnC binding region ($cTnI_{34–71}$ and $sTnI_{1–40}$) and a TnT2 binding region ($cTnI_{80–136}$ and $sTnI_{50–106}$), which completes N-cTnI [8]. The C-domain of cTnI (C-cTnI) includes an inhibitory region (Ir) that strongly binds actin ($cTnI_{128–147}$ and $sTnI_{96–115}$), a switch region (Sr) that strongly binds N-cTnC ($cTnI_{147–163}$ and $sTnI_{115–131}$), and a mobile domain (Md) that interacts either strongly or weakly with actin and Tm

(cTnI$_{164–210}$ and sTnI$_{132–180}$). Hence, in terms of structure, the "I" in TnI could just as well stand for "interactive" instead of "inhibitory."

The conformational plasticity of TnI makes its structural properties impossible to understand unless the influence of its binding partners is considered. Consistent with this propensity of TnI for protein–protein interaction, the conformational behavior of TnI puts the "switching" in CRS. The only persistently rigid regions within TnI are the C-TnC and TnT2 binding regions of TnI [60], which participate in forming the IT arm of the Tn core domain. However, this scaffolding role is important to CRS structure transitions, since *in vitro* H/D exchange and *in situ* anisotropy evidence suggests that the IT arm stabilizes Tn and localizes TnI to the Tf in a way that optimally positions the other TnI regions for their switchable protein interactions [20, 33, 60]. TheN-Ext-cTnI is directly attached to the C-TnC binding region of cTnI and it extends up cTnC to interact with N-cTnC when unphosphorylated [59]. This interaction may be switched "off" by PKA phosphorylation. FRET evidence suggests that the TnI-IR adopts a collapsed β-hairpin structure when bound to actin and a more extended conformation once switched by Ca^{2+}binding to N-TnC into interacting with TnC [61-63]. Ca^{2+}binding also switches cTnI-Md from a collapsed state [32] that strongly interacts with actin and Tm [7] into an unstructured, weakly interacting state [19, 64]. At the center of all this switching activity lies TnI-Sr, which is also called the switch peptide and regulatory region, and its ability to interact with N-TnC.

It was previously mentioned that the exposed hydrophobic patch of N-TnC facilitates interaction with a complimentary amphiphilic α-helix. Interestingly, the TnI-Sr exhibits a basic amphiphilic α-helix structural motif. This motif is the quintessential binding target of Ca^{2+}-bound CaM [43]. NMR verified that TnI-Sr interacts with the exposed hydrophobic patch of Ca^{2+}-saturated N-TnC [52, 65], and XRD demonstrated that the TnI-Sr takes on α-helical character when so bound [1, 2]. NMR [64, 66], FRET [67], and anisotropy [19] suggest that the TnI-Sr is less structured when dissociated from N-TnC. Thus, Ca^{2+} binding to N-TnC essentially switches "on" the TnI-Sr–N-TnC interaction, whereas Ca^{2+}-dissociation switches it "off." Like a master switch within a Boolean network, the conformational state of TnI-Sr thereby determines the ultimate conformations and protein–protein interactions of C-TnI's switchable protein regions. The TnI-Sr–N-TnC interaction is also the primary means by which the Ca^{2+}sensitivity of CRS can be modulated due to its energetic coupling with regulatory Ca^{2+} binding and N-TnC opening [68].

The ability of TnI-Sr to modulate N-TnC Ca^{2+}-binding affinity is just one example of how TnI can go beyond regulating force generation to influence the CRS process itself. This is made possible by TnI's higher degree of structural diversity than TnC, which is traced to the existence of N-Ext-cTnI in cardiac isoforms. NMR showed that N-Ext-cTnI can interact weakly with N-cTnC [69, 70]. This N-Ext-cTnI–N-cTnC interaction enhances the strength of the cTnI-Sr–N-cTnC interaction and thereby increases the Ca^{2+}-binding affinity of N-cTnC [71, 72]. An NMR study also suggested that the conformational state of N-Ext-cTnI can be changed to position its acidic N-terminus for interaction with cTnI-Ir [59]. These modulatory actions of N-Ext-cTnI are regulated by the effect of PKA-mediated PTMs made to Ser-22 and Ser-23 on the structure of TnI [59, 73]. Furthermore, PKC mediated PTMs of Ser-43, Ser-45, and Thr-144 (i.e., in *Mus musculus*) [74] were demonstrated through NMR and FRET [75] to also impact the N-Ext-cTnI conformation dominantly over PKA signaling [76]. cTnI also possesses a site at Thr-31 (i.e., in *H. sapiens*) that can be phosphorylated by

the apoptosis inducing Mst1 [77], and a site at Ser-151 (i.e., in *Rattus norvegicus*) that can be phosphorylated by p21-activated kinase [78] and AMP-activated protein kinase [79].

Lastly, when considering the basics of TnI structure, it is important to understand that its inhibitory action alone is inadequate for proper regulation of XB cycling. TnI is partnered with Tm in achieving the regulatory inhibition of muscular force generation over an entire Tf structural regulatory unit. Though TnI directly contacts Tm *via* the TnI-Md [7], an equally important indirect contact between Tm and TnI is mediated through TnT, the remaining Tn subunit yet to be discussed.

Troponin T

Originally envisioned as the scaffolding anchor of the Tn complex, structural studies have increasingly uncovered the important role of in TnT in CRS. TnT structure is remarkably similar to TnI structure and epitopic analysis has even detected evolutionarily suppressed TnI-like epitopes in TnT [80]. Like TnI, TnT is an elongated molecule that participates in numerous protein–protein interactions and whose N-terminus exhibits a high degree of structural diversity [81]. Unlike TnI, TnT contains a proteolytic cleavage site that divides the protein into two fragments upon mild chymotryptic digestion. The resulting N-terminal and C-terminal fragments are simply named TnT1 and TnT2, respectively. From the N-terminus, TnT1 structure begins with a hypervariable region (N-Var-TnT) that can be highly acidic and whose length can reach 70 residues depending on the vertebrate isoform [82]. Though N-Var-TnT currently has no structurally verified binding partner [81], its important functional roles in maximal Tf activation, Tf cooperativity, and Tm flexibility were recently biochemically identified [83, 84]. N-Var-TnT is followed by a ~81 residue conserved central region that interacts with the head-to-tail junction of axially joined Tm dimers through an N-terminal 39 residue Tm-binding region [38]. Thus, TnT not only anchors Tn to a single Tm dimer, but it also involves Tn in the allosteric coupling that occurs between axially adjacent regulatory units.

TnT1 is followed by the conserved ~100 residue TnT2 chymotryptic fragment that contains scaffolding functionality. The N-terminus of TnT2 contains a 25 residue Tm binding region that anchors Tn onto Tm [38]. This is followed by an extended region that binds N-TnI and C-TnC along its length and at its C-terminus, respectively, and thus integrates TnT into the core domain [81]. These structural properties of TnT2 indicate its important role in conformational signal transduction wherein it serves as the allosteric connection between CRS and Tm movement. Overall, TnT structure conceptually resembles an inverted, non-switching version of TnI with the extension region maintained at the N-terminus. The N-TnI and C-TnC binding behavior of the C-terminus of TnT2 is reminiscent of N-TnI, and the Tm binding sites in TnT1 and TnT2are reminiscent of the actin binding cTnI-Ir and cTnI-Md. These similarities are in keeping with the evolutionary divergence of TnT and TnI from a common ancestral protein to occupy unique functional niches in Tf regulation [80].

Like cTnI, cTnT contains PKC phosphorylation sites. Four locations have been identified: Thr-197, Ser-201, Thr-206, and Thr287 (i.e., in adult *H. sapiens*). The most functionally important site is Thr-206 [85], which is located close to the N-terminal cap of the α-helix that makes up the TnT2 outer prong of the IT arm W-scaffold. Computational simulation suggested that PKC-mediated phosphorylation of Thr-206 would extend the α-helix [85], which may somehow affect the conformational behavior of TnT; however, the mechanism remains unknown [86]. In contrast to TnI, TnT is not known to be

phosphorylated by PKA. Though TnT is highly regulated both developmentally and by restrictive proteolysis [81], the structural consequences of the associated modifications has not been characterized.

Interfacing between Troponin Subunits

As indicated above, TnC, TnI, and TnT are highly interactive proteins that act as an interdependent, integrated whole to regulate force generation *in vivo*. The integration of Tn subunits produces the Tn core domain (Fig. 1), which has been well visualized by XRD [1,2] and consists of the regulatory head anchored into the IT arm. The regulatory head (Fig. 1A) consists of N-TnC and the TnC central linker. The IT arm is built from the C-TnC- and N-TnI-binding regions of TnT2; the C-TnC- and TnT2-binding regions of N-TnI; and C-TnC, whose sites III and IV are constitutively bound to either Mg^{2+} or Ca^{2+} and whose hydrophobic patch is consequently exposed. The N-TnI-binding region of TnT2 and the TnT2-binding region of N-TnI are integrated as follows. TnT2 and N-TnI each fold into a helix-turn-helix motif wherein the C-terminal helix of the motif contains the binding domain. Thus, the C-terminal helices of each motif integrate into a coiled-coil. This results in a "W"-like scaffolding substructure (Fig. 1B) [2] somewhat resembling the head of a three-pronged kitchen fork, which for the convenience of further discussion will be named the "W-scaffold."

The base of the W-scaffold contains the turns of the TnT2 and N-TnI helix-turn-helix motifs. Further Tn integration is therefore accomplished by the "prongs" of the W-scaffold. One of the W-scaffold's outer prongs consists of the N-terminal portion of TnT2, and it thus binds to Tm [38]to directly anchor the W-scaffold onto the Tf (Fig. 1B). The central prong of the W-scaffold consists of the TnT2–N-TnI coiled-coil, and as Fig. 1B shows it is at the upper tip of this central prong where TnT2 interacts with C-TnC. The tip is also the point from where C-TnI projects out of the Tn core domain, which makes C-TnI well positioned for its switchable interactions with actin, Tm, and the Tn regulatory head. The W-scaffold's remaining outer prong consists of the N-terminal portion of N-TnI and projects toward C-TnC. In all vertebrate Tn isoforms, this remaining prong contains an amphiphilic α-helix that interacts with the exposed hydrophobic patch of C-TnC. C-TnC is thus "gripped" between the N-TnI outer prong and the central, coiled-coil prong of the W-scaffold (Fig. 1C) [2]. In cTn, N-Ext-cTnI also projects out from the tip of the N-TnI outer prong of the W-scaffold to interact with N-cTnC and the Ir in C-cTnI (Fig. 1B).

It is evident from this description ofthe W-scaffold that it couples Tn to the Tf and is important for organizing Tn subunits into a configuration optimal for actomyosin regulation. The spatial arrangement achieved by scaffolding facilitates additional interfacing between Tn subunits that involves the regional protein binding and dissociation events associated with CRS [87]. XRD has shown that when N-TnC is saturated with Ca^{2+}, TnI-Sr interacts with the exposed hydrophobic patch of open N-cTnC (Fig. 1D) [1, 2]. XRD of Ca^{2+}-saturated sTn has also shown that TnI-Ir interacts with a structured TnC central linker in the regulatory head [1, 2], a conclusion supported by neutron-scattering data showing that sTnC is extended when Ca^{2+} saturated [88-90]. However, it is notable that the TnC central linker and the TnI-Ir could not be visualized in the Ca^{2+} saturated cTn crystal structure. When N-sTnC was free of Ca^{2+}, it was in its closed conformation, the central linker of sTnC was melted, the interactions

between N-sTnC and C-sTnI were absent. The clear implication was that TnI-Ir would have switched to interacting with actin if it were present.

One remarkable facet of core domain structure is that in spite of the structural diversity found in vertebrate Tn subunits, the organization of Tn and the conformational behavior associated with CRS is very similar between sTn and cTn. In fact, some differences between the cTnC [1] and sTnC [2] crystal structures can be reconciled by considering the results of other studies. NMR [87, 91, 92], FRET [93], and H/D exchange [33] have showed that the cTnC central linker becomes more rigid when N-cTnC has Ca^{2+} bound in the presence of C-cTnI. NMR has also indicated that cTnI-Ir interacts with the TnC central linker under these conditions [92]. Finally, fluorescence anisotropy and amide H/D exchange have indicated that

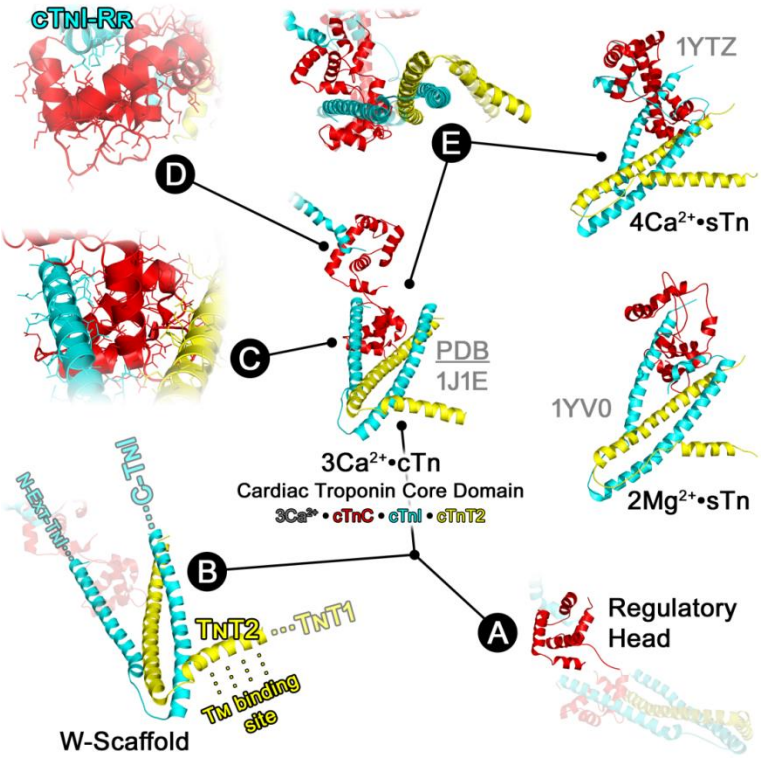

Figure 1. Shown here are various structural aspects of the Tn core domain based on the crystal structures produced by Takeda et al.[1] and Vinogradova et al. [2]. Crystal structures were rendered using PyMOL [94]. The entire Ca^{2+}-saturated cTn crystal structure is shown in the center of the diagram. Ca^{2+}-saturated sTn appears to the right of cTn, and Ca^{2+}-free sTn to the upper right, for comparison. A-E highlight important aspects of Tn subunit integration that are evident in the structures. **A)** The regulatory head is shown highlighted with the W-scaffold faded out. **B)** The W-scaffold of cTn is now highlighted with the regulatory head faded out. The relative locations of structural regions that were missing from the crystal structure are also indicated. **C)** This zoomed-in view depicts how the W-scaffold "grips" C-TnC *via* protein-protein interactions with N-TnI and TnT2. The exposed hydrophobic patch of C-TnC can be seen interacting with N-TnI on the left. **D)** Here, one can see how TnI-Sr interacts with the exposed hydrophobic patch of N-TnC under Ca^{2+} saturated conditions. **E)** Ca^{2+}-saturated cTn and sTn have been aligned here along the W-scaffold. Though the overall organization of the core domain is similar in both crystal structures, one can see minor differences in W-scaffold structure and how the significant structural differences between cTnC and sTnC affect the regulatory head and its interaction with TnI-Sr.

cTnI-IR is rigid under Ca^{2+} saturated conditions [19, 33], which further implies that it interacts with the cTnC central linker. When this additional evidence is considered, the most reasonable conclusion is that the unstructured nature of cTnI-IR and the cTnC central linker in the crystallized cTn core domain was due to the effects of crystal packing and missing binding partners on Tn structure [2].

In spite of their general structural similarities, there nevertheless are important, subtle differences between the organization of sTn and cTn core domains (Fig. 1E). The first and most obvious difference is the presence of the N-Ext in cTnI. NMR implicates residues 22-34 of this region as weakly interacting with the N-cTnC when unphosphorylated, which stabilizes the open conformation of N-cTnC [95, 96]. This interestingly suggests that the stabilizing effect of Ca^{2+} binding to site I [35], now missing due to evolutionary mutations, is being substituted to some extent with a switchable protein–protein interaction. Neutron scattering showed that compared to sTnC, cTnC is more compact yet less intertwined with other subunits when integrated into the core domain [97]. Though isoform specific structural differences do lead to subtle differences in the CRS mechanism that will be discussed later, the structural mechanism by which Tn subunits are integrated with each other is largely preserved.

Integration of Troponin into Thin Filament Architecture

We will now expand our scope to focus on the Tf, which is the macromolecular assembly in which Tn finds its most immediate *in vivo* molecular context. The Tf itself consists of F-actin with each strand decorated with coiled-coil Tm dimers and Tn complexes at regular intervals. The geometry involved gives rise to the sRU, which consists of seven actins bound to one Tm dimer and one Tn complex. EM has nicely shown how Tn is found at ~37 nm intervals along the Tf [32], and this periodicity matches the span of a seven-actin monomer stretch. A Tm dimer is ~42 nm [40], which allows axially adjacent Tm dimers to overlap, interact, and form a continuous strand that runs along F-actin [32]. Tm–Tm overlap interactions structurally consist of a flexible, interlocking head-to-tail junction that has been visualized by NMR [98]. Overlap junctions help maintain an alignment between Tm and actin optimal for Tm localization through its seven quasi-repeating motifs that weakly interact with the actin surface [98,99]. Therefore, Tn localizes to Tm through TnT1 and TnT2, and Tm is localizes to actin. Each strand of the Tf is thus built from a long chain of sRUs into which many Tn complexes are organized.

The structure of Tn when so incorporated into the *in vitro* Tf is consistent with its structure when in isolation and the structural effects expected from the presence of Tm and actin. Neutron scattering measurements of deuterated TnC incorporated into *Bos taurus* native myocardial Tfs suggested that TnC retains an extended dumbbell structure [100]. C-TnI structural regions that are dynamic in solution become structured in the presence of Tm and actin. FRET has indicated that the TnI-IR is collapsed into a helix-loop-helix motif when bound to actin in the relaxed state [63], and EM has shown that the TnI-MD is collapsed onto Tm and actin [101]. Anisotropy has provided supplementary observations that the TnI-IR and TnI-MD have low flexibility under relaxation, while the TnI-SR remains more flexible [19]. FRET has determined that the Ca^{2+}-dependent molecular distances between C-TnI functional regions, N-cTnC, and actin are consistent with the protein conformations expected during

CRS [6, 67, 78, 102, 103]. Interestingly, FRET has shown one perhaps unexpected structural effect of incorporating TN into the TF. In the absence of Ca^{2+}, the presence of actin causes the closed conformation of N-TNC to become more collapsed and increases the separation between TNI-SR and N-TNC [6]. PELDOR measurements have provided consistent observations [104]. This implies that a partial interaction between TNI-SR and N-TNC occurs when the TN complex is not incorporated into the TF, and that this partial interaction is prevented by the TNI-IR–actin and TNI-MD–actin interactions.

To further understand the effects of TF incorporation on the conformational behavior of TN, it is important to consider how TN becomes part of a greater ultrastructure. Lengths of randomly sampled TFs from papillary murine myocardium were determined by electron tomography and found to average 1.04 ± 0.03 μm (Fig. 2A) [105]. Each strand of these TFS would therefore contain ~27 sRUs, for a total of ~54 TN complexes organized into each murine TF. Rather than being in isolation, every TN complex thus is generally located next to three nearest neighbors. A neighboring TN is ~40 nm away on either axial side of aTN being considered, and a third neighbor is located ~8 nm radially away on the other lateral side of the TF (Fig. 2D). Conformational changes inTF-incorporated TN thus occur under the possibility of structural influence from neighboring TNs. The orientation of TN with respect to the actin surface also becomes structurally relevant because TN is anchored to TM and TM position changes during CRS. Cryo-EM suggested that TN–TM is located on the outer actin domain under relaxing conditions, and moves azimuthally around the lateral actin surface to the inner actin domain when Ca^{2+}-saturated [106]. Since the switching state and azimuthal position of each of the ~54 TN complexes in a TF is determined by a combination of sarcomeric Ca^{2+} level, TF architecture, and stochastic molecular motion, even an *in vitro* reconstituted TF becomes quite complicated.

The potential the TF ultrastructure creates for allosteric communication between TF-incorporated TN complexes imbues the conformational behavior of Tn with a high degree of cooperativity. This is clearly seen under the *in situ* setting, wherein the steady state relationship between force generation and sarcomeric Ca^{2+}levels is described by a Hill coefficient that is consistently reported to be3–4[107]. This is surprisingly steep, since TN contains two regulatory Ca^{2+} binding sites at most. Such steepness suggests that CRS is cooperatively triggered by Ca^{2+} in a manner requiring allosteric communication between neighboring TN complexes. Axially directed allosteric communication (Fig. 2D) occurs because each TN is allosterically coupled with its axial neighbors through its TNT subunit and TM head-to-tail junctions. Furthermore, the persistence length of TM is sufficient for facilitating axial allostery between neighboring sRUs[108], and saturation transfer EPR has shown that actin and TN exert a rigidifying effect on TM such that TM backbone dynamics are not a major factor in TM movement during CRS and sXB binding [109]. Similarly, it is now understood that TM is azimuthally braced between radially neighboring TNs under relaxing conditions [32,106], which may represent another pathway for allosteric communication (Fig. 2D). TF CRS thus involves a high degree of allostery mediated by numerous protein–protein interactions which occur over impressively long molecular distances.

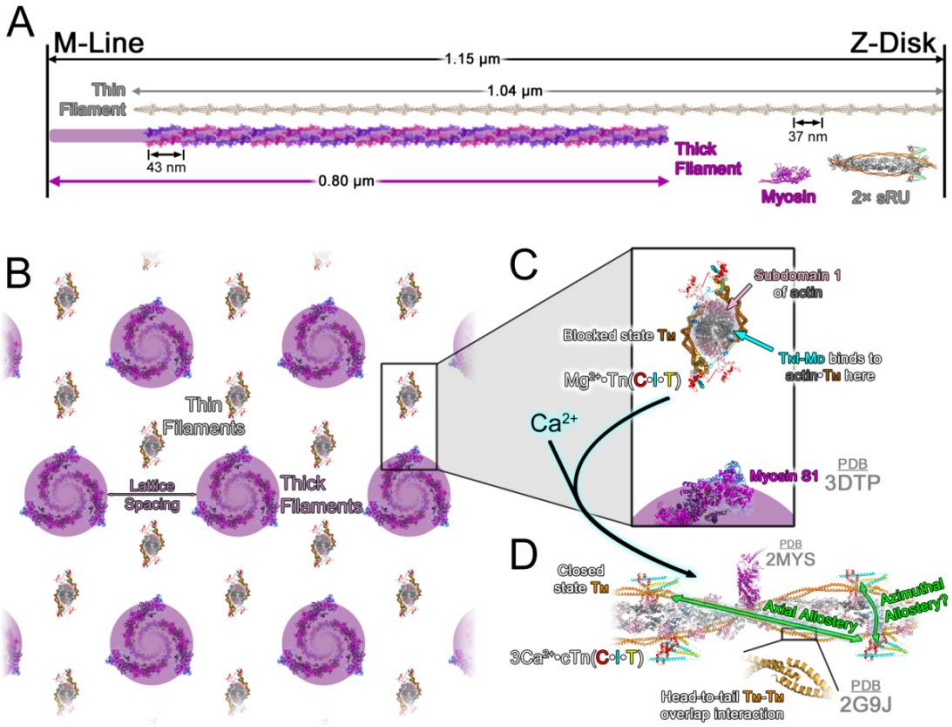

Figure 2. This figure presents the ultrastructural context that TN experiences once it is integrated into the TF. The protein structures seen in this figure are from the indicated PDB coordinate files rendered using PyMOL [94]. The exception to this is that all TF protein structures were rendered from supplementary data provided by Hoffman et al. [64]. **A)** Shown here is a model of a single TF overlapping with a single thick filament at a sarcomere length of 2.3 μm. The indicated lengths of the thin [105] and thick filaments [110] are based on measurements that have been made by Burgoyne *et al.* and Kensler, respectively, using EM. One can see from the diagram how the TF consists of a coiled-coil built from strands of sequential repeats of ~37 nm long sRUs. The rendered myosin heads shown in the thick filament cartoon depict how thick filament architecture results in coils of myosin molecules wherein myosin heads are oriented for interaction with neighboring TFs. The structural arrangement shown is based on the measurements made by AL-Khayat et al. using EM and single particle analysis [111]. The axial spacing between crowns of myosin heads is ~14.3 nm [112], and the azimuthal orientation with which a myosin head projects out of the thick filament is repeated every ~43 nm [110, 111]. **B)** The model in panel A is flipped to an end-on view looking down the central axes of the filaments and expanded to depict a sarcomere lattice. As in panel A, the myosin head structures shown in the thick filaments depict head projection points based on EM [110, 111] and a stereospecific model by Suzuki et al. [112]. **C)** A thin and thick filament from panel B are shown in a close-up view looking down their filament axes. One can see how TN–TM sterically blocks the myosin binding sites found on the outer actin domain [113]. TM position is controlled by a pair of TN complexes working together across the lateral surface of F-actin such that TM is sandwiched in place between TnT and TnI [32]. **D)** The TF from panel C is now viewed laterally under Ca^{2+}-saturated conditions with a XB about to strongly bind actin. This diagram thus emphasizes the potential for allosteric communication between neighboring TN complexes during activation. Axial allostery between the TNs of neighboring sRUs is mediated through TM–TM overlap interactions [98, 108] known to interact with TnT1 [38, 83, 84]. Azimuthal allostery may also be possible due to the counterpunching mechanism of TN-mediated TM positioning. Since S1 also controls the position TM on actin [114, 115], there is the potential for both TF intrinsic and sXB mediated allosteric effects on CRS [107, 116].

Structural Basis of Role in Interactions between Thick and Thin Filaments

Until now, structural details of the process regulated by TN-mediated CRS have yet to be considered in this chapter. That process is the interaction between thin and thick filaments that culminates in force generation (Fig. 2). In order to understand the structural relationship between TN conformational behavior and sXB formation, the ultrastructure of the sarcomere must be considered once again. TFs are assembled from their anchoring point in the Z-disk of the half-sarcomere, which is a scaffolding macromolecular assembly built from numerous proteins including α-actinin, CapZ, desmin, etc. [39]. TFs extend toward the M-line of the half-sarcomere, which is another scaffolding macromolecular assembly built from myomesin, M-protein, etc., into which thick filaments are anchored. The giant, spring-like ruler protein titin connects the Z-disk to the M-line, and myosin-binding Protein-C provides a radial connection between thick and thin filaments [111]. Thus, the TF possesses a spatial relationship with surrounding thick filaments at all times in the physiological myocyte. It is the structural consequences of this spatial relationship on TF regulation and force generation that give sarcomere length (Fig. 2A) and lattice spacing (Fig. 2B) their physiological significance [117, 118].

Thick filaments are primed for interaction with the TFs. Vertebrate thick filaments are built from three-headed crowns of myosin molecules [111, 112]. In each crown, myosin heads project out of the thick filament lateral surface at 0°, 120°, and 240° degrees around the thick filament axis in an internal frame of reference (Fig. 2B). Crowns are stacked with a ~14.3 nm periodicity such that each successive crown is rotated ~40° around the thick filament axis; however, it should be noted that the thick filament does not conform to an exact, unperturbed helical arrangement according to EM evidence [111]. Since a sarcomere unit lattice has a hexagonal arrangement (Fig. 2B), a TF will "see" a myosin head whose lateral orientation is optimal for actin binding every ~43 nm. However, every ~14.3 nm there is a myosin head whose lateral orientation permits some chance of binding actin. The result as far as TN is concerned is that many myosin heads are readily available for binding actin along a significant length of the TF (Fig.2A). TN is able to block the onrush of myosin binding and force generation through its regulatory partnership with TM (Fig. 2C).Under relaxing conditions, TN–TM occupies a position on the outer domain of actin wherein myosin binding sites are sterically blocked [113]. Optical laser trap measurements have suggested that this blocking position of TN–TM reduces the rate of sXB attachment by ~100× [37]. Interestingly, EM evidence has also suggested that the blocked state TM position is locked in place by azimuthally paired TN complexes working across the actin surface in what has been described as a counterpunching mechanism [32, 101, 106].

There are some notable idiosyncrasies in the structural relationship between thin and thick filaments. For example, their mismatch in periodicity is particularly interesting. An optical laser trap study demonstrated that myosin heads bind native *in vitro* TFs with distances of either 36, 72, or 108 nm between bound heads [112]. Furthermore, EM measurements in IFM have shown that sXB attachment predominantly occurs toward the center of a sRU [119].This indicates that myosin binding to actin occurs according to TN–TM and not thick filament periodicity and implies that only one myosin head can be bound to an sRU at a time. It also suggests that the fully activated TF may not necessarily be saturated with XBs *in vivo*. In fact, due to the nature of myofilament lengths and arrangements, approximately one third of the TF does not even overlap with the XB-bearing zone of the

thick filament (Fig. 2A). Another interesting facet of the structural relationship between TN and myosin is the ability of sXB attachment to cause Ca^{2+}-sensitizing changes in TN conformation in what is termed the "positive feedback mechanism"[107,120,121]. Since myosin itself moves TM, and TN is so intimately associated with TM, myosin-induced TM movement affects TN conformational behavior. Numerous *in vitro* reconstituted TF and *in situ* studies have in fact observed S1-induced effects on changes to TF allostery (Fig. 2D) and changes in N-TNC structure consistent with Ca^{2+}-sensitization [6, 19, 21, 36, 67, 102, 103, 122].

Changes in Troponin Conformational States

In the preceding sections, we have discussed how various structural methods have elucidated the structural arrangement and stable conformations of TN when incorporated into the TF. We have thus laid the groundwork for discussing the advances in our contextual and mechanistic understanding of how TN conformational changes occur during CRS. This is the most advanced aspect of TN structural study. The highly allosteric regulatory conformational behavior of TN involves conversions between stable conformations, and such conversions entail energetics, dynamics, and kinetics. This makes CRS an impressively tunable mechanism for regulating muscular force generation. However, it also means that seemingly innocuous residue substitutions can have serious pathophysiological consequences for the molecular mechanism underlying CRS. Therefore, characterizing physiological CRS is an important scientific goal.

Though *in vivo* CRS behavior is incredibly complex, our field has made considerable advancements in building a more accurate and dynamic structural picture of this exquisite evolutionary adaptation of Ca^{2+} regulation for controlling muscle contractility. Many biophysical insights into the molecular mechanisms underlying CRS have been gained. We will begin by exploring what has been learned about how CRS itself starts: with the binding of Ca^{2+} to N-cTNC.

Ca^{2+} Binding and Opening of the N-domain of Troponin C

The binding of Ca^{2+} to N-TNC supplies the energy needed for TN to begin converting from its stable force-inhibitory conformation into an activating conformation that permits force generation [35, 68]. This energy input is required for exposure of the N-TNC hydrophobic patch to solvent and concomitant access by TNI-SR. The conformational behavior of TNC is thus energetically tuned for converting a Ca^{2+}-signal into a cascade of conformational changes within TN. This energetic tuning is complex. For example, Ca^{2+} binding to sites I and II are unequal energetic contributors to the N-sTNC opening process. NMR has shown that Ca^{2+} binding occurs in a stepwise manner first to site II followed by site I [123]. Furthermore, circular dichroism has indicated that Ca^{2+}-binding to site II plays the dominant role in opening N-sTNC, whereas site I stabiles the open conformation [35]. Interestingly, the ability of N-cTNC site II to stimulate similar changes in Ca^{2+}-dependent ellipticity was attenuated relative to N-sTNC site II, suggesting that N-cTNC site I was not

merely disabled but was hampering N-cTnC opening by site II on some level. This evolutionary energetic tuning significantly affects TN conformational behavior.

One of the more fascinating isoform-specific differences between sTnC and cTnC is how the Ca^{2+}-dependent conformational conversion process involved in the CaM-like opening of the N-domain occurs. sTnC behaves as would be intuitively expected. Ca^{2+} binding to sites I and II of sTnC opens up N-sTnC, which stably exposes an interaction site that triggers CRS through TnI-Sr. It turns out that site I in N-cTnC is not only disabled, but also mutated to introduce an additional entropic cost for opening N-cTnC [35]. This ensures that N-cTnC will not stably open upon Ca^{2+} binding to site II [50, 51, 53]. However, the Rosevear lab demonstrated through NMR that N-cTnC undergoes a partial opening [124]. This was later elaborated on by the Sykes lab, who showed that this partially open conformation involves a mere ~36 $Å^2$ increase in the solvent exposed surface area of the N-cTnC hydrophobic core[125]. This is compared to the ~554 $Å^2$ increase in surface area experienced by N-sTnC [15]. FRET measurements also indicated that no major intra domain distance increases occur in N-cTnC unless cTnI-Sr is present [53]. Hence, unlike N-sTnC, both Ca^{2+} and cTnI-Sr are needed for N-cTnC to stably enter the open conformation.

The fact that simultaneous Ca^{2+} binding and cTnI-Sr interaction are needed for N-cTnC opening may seem like a mechanistic paradox. If Ca^{2+} represents the signal that is supposed to trigger the cTnI-Sr–N-cTnC interaction and subsequent CRS, what happens when Ca^{2+} can't open N-cTnC on its own? Strong evidence toward an answer was recently provided by a paramagnetic relaxation enhancement NMR study by Cordina et al. conducted on isolated, spin labeled cTnC [126]. N-cTnC was shown to exist in an equilibrium between its opened and closed conformations. This finding is in agreement with interpretations made in past NMR studies [69, 127, 128] and FRET studies from our lab [6, 129, 130]. Cordina et al. observed that when Ca^{2+} was absent, the N-cTnC conformational equilibrium was dominated by the closed conformation. Ca^{2+} binding partially stabilized the open conformation, which shifted the equilibrium enough to create a probabilistic opportunity for the cTnI-Sr to access the N-cTnI hydrophobic core. Once Ca^{2+} and cTnI-Sr were both bound to N-cTnC, the N-cTnC conformational equilibrium became dominated by the open conformation. The evolutionary disabling of N-cTnC site I thus leads to a conformational selection mechanism for the exposure of the N-cTnC hydrophobic patch. This implies that sTn and cTn rely on the same fundamental TnI-Sr dependent CRS mechanism to achieve TF regulation.

Switching of the C-domain of Troponin I

Once the CRS is triggered by the N-TnC Ca^{2+}binding or dissociation, the switching of the protein–protein interactions of C-TnI represents the next step in the conformational conversion mechanism. Ca^{2+}-binding kinetics are extremely rapid, with an apparent bimolecular rate constant of 5.1×10^7 $M^{-1}\cdot s^{-1}$ for binding to the whole complex at 4 °C. However, the conformational changes associated with CRS progress at much slower rates and follow a defined series of events in which C-TnI is heavily involved. The biophysical principle underlying the role of C-TnI in CRS is that of energetic balance. Ca^{2+}-binding to N-TnC and TnI-Sr's interaction with the exposed hydrophobic patch of N-TnC work together against an energetic "counterweight" in the form of the TnI-Ir–actin and TnI-Md–actin

interactions to control the overall conformational behavior of TN in effecting TF activation and deactivation.

Thin filament Activation

Structural evidence strongly indicates that a sRU is activated by CRS through what is known as the "drag and release" mechanism [6,19]. The sRU begins in the relaxed state; TN is anchored *via* TNT2 and TNT1 onto the rigid TM dimer of the sRU [109]. The rigid IT arm is holding the regulatory head close to the actin surface in a position optimal for interaction with TNI-SR and therefore the triggering of CRS [20]. The TNC central linker is melted. TNI-IR and TNI-MD are bound to actin [67,102]and thus inflexible [5, 19, 60], whereas the TNI-SR is unbound, disordered, and rapidly sampling the space near N-CTNC [64]. TNI-MD is also interacting with the TM dimer of the cross-filament sRU [32, 131]. Ca^{2+} first rapidly binds to N-TNC. This causes stable hydrophobic patch exposure in N-STNC, whereas in N-CTNC the conformational selection mechanism is initiated [126]. The flexible TNI-SR stochastically encounters and recognizes the exposed hydrophobic patch and collapses into a strong interaction with N-TNC that stabilizes N-TNCin the open conformation. The interaction between Ca^{2+}-saturated N-TNC and TNI-SR "drags" TNI-IR and TNI-MD out of interaction with actin. This "releases" TNI-IR and TNI-MD from actin, which causes the TN-mediated confinement of TM in the blocked-state position to cease. TM spontaneously moves toward the inner domain of actin to occupy an energetically minimized closed-state position [115], which releases the inhibition of force generation. TNI-IR switches to interacting with the central linker of TNC, which stabilizes the linker into a more rigid conformation. Finally, the TNI-MD becomes flexible, but maintains cross-filament transient contacts with its TM binding partner [64].

FRET measurements of reconstituted thin filaments mixed with Ca^{2+}*via* stopped flow suggested that a three-step kinetic mechanism underlies the N-CTNC opening transition required for triggering the drag and release mechanism [132, 133]. The first step was too fast to be resolved, but the other two steps were slower. These observations suggested that N-TNC experiences an initial rapid and dramatic opening, followed by more modest and slower structural changes. Based on the TF deactivation mechanism to be discussed next, it is likely that the fast step relates to the folding of previously unstructured CTNI-SR into an interaction with the exposed hydrophobic patch of N-TNC. The slow steps then likely represent conformational changes associated with the drag-and-release mechanism triggered by the TNI-SR–N-TNC interaction. Whether the kinetics of the drag-and-release mechanism can rate-limit force generation is a point still being debated. While some studies seem to have ruled out the possibility that the kinetics of TF-activating TN conformational changes can be rate limiting [134], a recent study by Kreutziger et al. has suggested that the possibility exists when certain mutations are present within TN subunits [135].

Thin filament Deactivation

TF deactivation does not occur as a symmetric reversal of activation. The best structural evidence indicates that a sRU is deactivated by CRS through what is called the "fly-casting mechanism" [64]. Fly-casting refers to a conformational behavior of TNI-MD wherein it maintains periodic contacts with TM on the actin surface during its rapid conformational sampling under Ca^{2+}-activated conditions. When Ca^{2+} dissociates from TNC, weakening of the N-TNC–TNI-SR interaction allows TNI-MD to rapidly refold into its binding interaction

with actin–TM. This rapid collapsing of TNI-MD back down onto the actin surface helps to further destabilize the TNI-SR–N-cTNC interaction, and TNI-IRis eventually pulled out of interaction with the TNC central linker and back down onto actin. TM is moved to the blocked position concomitantly with the return of C-TNI to the surface of actin. The TNI-MD is thus thought to serve as an accelerator of relaxation.

There is strong empirical support for the fly-casting mechanism from the kinetic studies of *in vitro* TF deactivation. Time-resolved anisotropy measurements have demonstrated differences in the rates of changes in C-cTNI regional protein dynamics that match the predictions of the fly-casting mechanism[19]. Changes in the regional dynamics of cTNI-MD as induced by Ca^{2+} dissociation were the most rapid, followed by changes in the cTNI-SR and then cTNI-IR. FRET has also indicated that the kinetics of changes in the distance between each of these structural regions and cTNC, as induced by Ca^{2+} dissociation, follow the same pattern [103]. A recent H/D exchange study has implicated the dynamic regions of TN as prominently involved in CRS [5], which is a key implication of the fly-casting mechanism. Finally, an EM study showed that truncation of the C-terminus of cTNI-MD destabilized closed-state TM, suggesting that TNI-MD normally makes stabilizing contacts with closed-state TM as predicted by the fly-casting mechanism [131].

The debate over whether the kinetics of TF conformational changes can rate limit the kinetics of contractility also extends to relaxation [134]. An *in situ* kinetics study weighed in on this issue using an environmentally sensitive fluorophore to measure the N-sTNC Ca^{2+} dissociation rate in psoas muscle from *Oryctolagus cuniculus* [16]. The study demonstrated that the Ca^{2+}-dissociation rate matched the rate of force relaxation. Interestingly, another *in situ* environmentally sensitive fluorescence study on ventricular myofibrils from *O. cuniculus* showed evidence that at physiological temperatures, CRS and XB cycling might be kinetically similar[17].

Movement of Tropomyosin

The ultimate functional purpose of CRS is to control the position of TM on the actin surface. However, we have already alluded to the interdependent structural relationship between TM movement and CRS. The three-state model of TM positioning provides the basis for understanding how CRS and TM movement are structurally intertwined [113]. As mentioned previously, blocked-state TM covers myosin binding sites on the outer domain of actin and sterically blocks the attachment of sXBs. Closed-state TM is moved toward the actin inner domain and leaves myosin binding sites partially uncovered. As far as CRS is concerned, TN regulates TM occupancies of the blocked-and closed-state positions. As far as TM is concerned, the closed state is its "natural" location on actin [115]. Open-state TM is moved even further into the act in inner domain due to the formation of a sXB that pushes TM out of the way and thereby completely uncovers the myosin binding sites of the sRU. Such XB-induced movement of TM inevitably impacts TN structure. Labeled TN exchange in *O. cuniculus* myofibrils suggested that the three different states of TM produced three states of TN [136]. Along different lines, EM has shown that increasing the affinity of TM for actin will actually reduce the affinity of myosin for actin. Thus, the mutual interaction of TN, TM, and myosin with the actin surface involves an important energetic balance. Along similar lines, troponin counterpunching [32] recognizes that a mutual balance exists between cross-filament

neighboring sRUs that work together to control the position of their respective TM dimers. That a sXB induced change in the position of TM can control the conformation of TN is the idea that led to the proposal of a reversible fourth state of TF regulation [116].

Fourth State of Thin Filament Regulation

When Ca^{2+} dissociates from an activated sRU, the fly-casting mechanism is expected to pull TNI-SR and TNI-IR off of TNC and down onto the actin surface. Ideally, TM will be moved and confined to the blocked state during this process. However, what if myosin is already bound to the sRU and blocking interaction between CTNI and actin? The answer to that question is the reversible fourth state of TF regulation as proposed by Sherwin Lehrer [116]. The concept underlying the fourth state is that there are times during physiological muscle function wherein a sXBs will activate an sRU even though N-TNChas no Ca^{2+}bound to it. The associated removal of conformational constraints on TNI-SR should indirectly promote the Ca^{2+}-sensitizing TNI-SR–N-TNC interaction[19]. The consequence is that the affinity of N-TNC for Ca^{2+}will be significantly enhanced in the fourth state because the unconstrained TNI-SR stabilizes the open N-TNC conformation optimal for Ca^{2+}chelation [116, 130].

Troponin Counterpunching

The sRU is typically thought to regulate its own capacity for myosin binding. EM measurements have turned this notion on its head by showing that sRUs work as cross-filament pairs to regulate TM position across the lateral surface of actin [32, 101, 106]. One cross filament neighbor binds TM with its TNT2 region on one side, whereas the TNI-MD of the other cross-filament neighbor is collapsed onto actin and TM on the other side (Fig. 2C). TM is therefore laterally sandwiched between two TN complexes in the blocked-state position. This raises several interesting mechanistic structural questions that warrant further investigation. For example, say that Ca^{2+} binds to the N-TNC of one sRU in a cross-filament pair, which we will call $(TN–TM)_1$. $(TN–TM)_1$ will then undergo CRS and its TNI-MD will unbind actin and therefore no longer constrain the TM of the other, Ca^{2+}-free sRU of the pair, which we will call $(TN–TM)_2$. Interestingly, the azimuthal direction that newly Ca^{2+}-saturated $(TM–TN)_1$ must move in traversing from the blocked-state position to the closed-state position is in the direction of the still-collapsed and actin-bound TNI-MDof Ca^{2+}-free $(TM–TN)_2$. How these events would thus impact the conformational state of $(TM–TN)_2$ is unknown, but it is reasonable to hypothesize that TN counterpunching represents an azimuthal pathway for allosteric communication that is likely Ca^{2+}-sensitizing.

Structural Effects of Strong Cross-bridge Attachment

One of the more surprising properties of CRS is that the very process it regulates, the actomyosin XB cycle, has the ability to regulate CRS through the positive feedback mechanism. Positive feedback complicates our understanding of how CRS and TM movement occur *in vivo*. The fact that Ca^{2+}-saturated TN undergoes conformational changes as TM moves to the open position suggests that sXBs exert important structural effects on TN that are additional to the effects of Ca^{2+}-binding. Numerous lines of *in vitro* and *in situ* biophysical evidence have borne this out.

Ca^{2+}-Sensitizing Structural Feedback

It has long been known that the attachment of sXBs to the TF enhances the Ca^{2+}sensitivity of N-TNC through the positive feedback mechanism [120]. As structural evidence has accumulated, the molecular mechanism that underlies positive feedback has become clearer. *In vitro* FRET studies have shown three key pieces of evidence. First, the attachment of sXBs to the TF causes Ca^{2+}-bound N-CTNC to adopt a more open conformation and increasesCa^{2+}-sensitivity [133]. Second, the distance between TNI-SR and N-TNC decreases [6]. Third, the distance between TNI-SR and actin increases [67]. Taken together, these results suggest that sXB attachment exerts a Ca^{2+}-independent stabilizing effect on the TNI-SR–N-TNC interaction by releasing the conformational constraints that are placed on the TNI-SR when the TNI-IR and the TNI-MD are interacting with actin. That this mechanism occurs *in situ* was supported by the work of Sun *et al*. that showed how E-F hand helix orientation in CTNC has both Ca^{2+}- and myosin-dependent components, and how the presence of sXBs was Ca^{2+}sensitizing [21]. It was later confirmed by Rieck et al. [130] using *in situ* FRET in skinned myocardial fibers that the structural basis for the positive feedback is sXB-mediated stabilization of the Ca^{2+}-sensitizing TNI-SR–N-TNC interaction. This stabilization increased the ensemble-averaged FRET distance associated with the open conformation of N-CTNCby ~1.4-fold. Due to the nature of ensemble FRET measurements, it is still unclear whether sXB-mediated stabilization causes the open conformation of N-TNC to open up further, or whether Ca^{2+}-saturated N-TNC is in a conformational equilibrium that is shifted further toward the open conformation.

Role of Cross-Bridges in Thin Filament Cooperativity

The role of sXBs in cooperative TF activation has recently fallen under renewed scientific scrutiny. It was long thought that the high degree of steepness observed in the force-Ca^{2+} relationship of myocardial and fast-skeletal vertebrate muscle was due to sXB positive feedback [107]. This is a reasonable hypothesis, since the energy of the XB-induced movement of TM in one sRU can be expected to transmit itself into neighboring sRUs *via* TM–TM overlap interactions. Seminal biochemical studies had shown that exposure of skinned muscle to a strong-binding derivative of myosin subfragment-1 (NEM-S1) attenuated the cooperativity of Ca^{2+}-dependent activation [120]. Since NEM-S1 competitively inhibited sXB formation, sXBs were hypothesized as the missing component whose presence would normally drive allostery. However, more recent structural studies have presented evidence that requires this hypothesis to be reevaluated.

In situ anisotropy of bifunctional rhodamines attached to N-CTNC [20] and FRET measurements of N-CTNC opening [130] have both shown that the Ca^{2+}-dependent opening of N-CTNC occurs steeply when sXB attachments are absent. When blebbistatin or vanadate were used block sXBs, N-CTNC opening in response to Ca^{2+}binding occurred as steeply as myocardial force generation under conditions of cycling XBs, albeit with a reduced Ca^{2+}sensitivity. Furthermore, while the cooperativity of N-CTNC opening was blunted by non-cycling sXBs in sRUs located in the XB-bearing zone of the half-sarcomere, N-CTNC opening still occurred steeply in the XB-free zone where sXBs could exert no influence. Another *in situ* structural study used linear dichroism to observe that the majority of the structural changes that occur in CTNC are triggered by Ca^{2+} alone [36]. Importantly, vanadate had no significant effect on the steepness of CTNC structural changes either in study in question, or in another study employing *in situ* anisotropy [137].

These observations imply that the capacity for cooperativity in TF activation is a property intrinsic to the TF itself [107,130] and fits well with current knowledge of CRS. The energy of TM movement in one sRU, whether induced by Ca^{2+} or myosin, should be transmitted through TM–TM overlap interactions into any its neighboring sRUs that are switched off [108]. Given the possible allosteric effects of counterpunching during CRS, cross-filament allostery may also play a role. Whatever allosteric communication pathways are involved, energy transmitted into neighboring sRUs should promote TM movement and thereby produce Ca^{2+}-sensitizing structural feedback on TN. Since cTNC is especially sensitive to energetic modulation [126], this may explain why the cardiac CRS mechanism is more dependent on allosteric communication than the skeletal mechanism [138, 139].

Possibility of Structural Effects from Weakly Bound Cross-Bridges

Since myosin can weakly bind to the TF, whether weak XBs can promote TM movement or changes in TN structure is an important scientific question that is still under investigation. Since myosin binding strength is a key source of energy required for moving TM to the open position [37,115,140], it seems unlikely that weak XBs would be a major contributor to TM movement. Structural evidence has recently showed that weak XBs are at least unable to move TM to the open position. *In situ* anisotropy and blebbistatin have showed that cycling XBs exert effects on N-cTNC α-helix orientation additional to changes induced by Ca^{2+}[21]. Rigor XBs produced further structural feedback effects on cTN. Such XB-dependent structural changes would be very difficult to explain if weak XBs had already promoted TM fully to the open position. Evidence from XRD in *Lethocerus indicus* IFM was more direct. While Ca^{2+}-binding to TN was shown to move TM from the blocked to closed states, vanadate-induced weak XBs could not detectably impact the position of closed-state TM on the actin surface [141]. However, it has not yet been conclusively shown that weak XBs have no impact whatsoever on the energy landscape associated with CRS and TM movement.

Switching Concept of Post Translational Modifications

It was mentioned earlier in the chapter how N-Ext-cTNI interacts with N-cTNC and boosts its Ca^{2+}sensitivity. It has been suggested in a paramagnetic relaxation enhancement NMR study that N-EXT-TNI exerts its Ca^{2+}-sensitizing effect on N-cTNC by shifting its conformational equilibrium toward the open state and thereby enhancing the conformational selection mechanism [69, 126]. NMR data supports this notion by having shown that N-EXT-TNI enhances N-cTNC affinity for cTNI-SR and not Ca^{2+} directly [72]. This view is also supported by NMR measurement of the effect of phosphorylation on the binding affinity of N-cTNC for cTNI-SR [71]. PKA-mediated phosphorylation of sites Ser-23 and Ser-24 introduces a bend into the N-EXT-TNI that switches it from interacting with N-cTNI to interacting with TNI-IR via its acidic N-terminus [59, 73, 142]. What these structural observation simply is that the N-EXT-cTNI is an additional switching system that evolution has added onto the TN molecular switch to provide the cardiomyocyte even more control over force generation.

Conclusion

The TN-mediated CRS mechanism for regulating muscular force generation is truly a complex and amazing evolutionary achievement. As a field, we have progressed from trying to understand whether N-cTNC even opens as part of regulation to exploring its structural modulation by a variety of pathways. We are now characterizing TN structure *in situ*, measuring the kinetics of conversions between conformations, determining TN dynamics, and elucidating previously obscured molecular mechanisms. Nevertheless, the careful experimentalist should always be at least a little haunted by the reality that the observation of TN structure paradoxically requires its perturbation and decontextualization to some degree. The key to continued advancement in our field is that no particular approach is inordinately trusted. Rather, the field of TN structure is at its best when it is both self-critical and, like TN itself, collaborative. The intricate complexity of *in vivo* TN conformational behavior defies easy exploration. We may thus gain confidence in our observations and interpretations only as knowledge is steadily accumulated from numerous lines of investigation. Many exciting advances remain on the horizon for us to pursue in our scientific quest to understand the physiological conformational behavior of TN.

Acknowledgments

The authors would like to thank Murali Chandra for helpful discussions regarding the content and scope of the chapter narrative. We are also grateful to J.P. Jin for his assistance with the narrative. The authors were supported by NIH grant number R01 HL80186-5S1 and Award Number T32GM008336 from the NIGMS during the preparation of this book chapter. The content is solely the responsibility of the authors and does not necessarily represent the official views of the National Institute of General Medical Sciences or the National Institutes of Health.

References

[1] S. Takeda, A. Yamashita, K. Maeda, Y. Maeda, *Nature* 424 (2003) 35-41.
[2] M.V. Vinogradova, D.B. Stone, G.G. Malanina, C. Karatzaferi, R. Cooke, R.A. Mendelson, R.J. Fletterick, *Proc Natl Acad Sci U S A* 102 (2005) 5038-5043.
[3] S.Y. Boateng, P.H. Goldspink, *Cardiovasc Res* 77 (2008) 667-675.
[4] W. Dong, S.S. Rosenfeld, C.K. Wang, A.M. Gordon, H.C. Cheung, *J Biol Chem* 271 (1996) 688-694.
[5] D. Kowlessur, L.S. Tobacman, *J Biol Chem* 287 (2012) 42299-42311.
[6] J.M. Robinson, W.J. Dong, J. Xing, H.C. Cheung, *J Mol Biol* 340 (2004) 295-305.
[7] Z. Zhang, S. Akhter, S. Mottl, J.P. Jin, *FEBS J* 278 (2011) 3348-3359.
[8] M.X. Li, X. Wang, B.D. Sykes, *J Muscle Res Cell Motil* 25 (2004) 559-579.
[9] B. Bullard, A. Pastore, *J Muscle Res Cell Motil* 32 (2011) 303-313.
[10] E. Ehler, M. Gautel, *Adv Exp Med Biol* 642 (2008) 1-14.

[11] M.F. Patterson, D.G. Stephenson, *Pflugers Arch* 440 (2000) 745-750.
[12] T.C. Irving, J. Konhilas, D. Perry, R. Fischetti, P.P. de Tombe, *Am J Physiol Heart Circ Physiol* 279 (2000) H2568-2573.
[13] S.M. Harrison, D.M. Bers, *J Gen Physiol* 93 (1989) 411-428.
[14] J.R. Lakowicz, Principles of fluorescence spectroscopy, *Springer*, New York, 2006.
[15] N.C. Strynadka, M. Cherney, A.R. Sielecki, N.C. Strynadka, L.B. Smillie, M.N. James, *J Mol Biol* 273 (1997) 238-255.
[16] S.C. Little, S.B. Tikunova, C. Norman, D.R. Swartz, J.P. Davis, *Front Physiol* 2 (2011) 70.
[17] S.C. Little, B.J. Biesiadecki, A. Kilic, R.S. Higgins, P.M. Janssen, J.P. Davis, *J Biol Chem* 287 (2012) 27930-27940.
[18] W.J. Dong, C.K. Wang, A.M. Gordon, H.C. Cheung, *Biophys J* 72 (1997) 850-857.
[19] Z. Zhou, K.L. Li, D. Rieck, Y. Ouyang, M. Chandra, W.J. Dong, *J Biol Chem* 287 (2012) 7661-7674.
[20] A.C. Knowles, M. Irving, Y.B. Sun, *J Mol Biol* 421 (2012) 125-137.
[21] Y.B. Sun, F. Lou, M. Irving, *J Physiol* 587 (2009) 155-163.
[22] R.E. Ferguson, Y.B. Sun, P. Mercier, A.S. Brack, B.D. Sykes, J.E. Corrie, D.R. Trentham, M. Irving, *Mol Cell* 11 (2003) 865-874.
[23] J.M. Robinson, W.J. Dong, H.C. Cheung, *J Mol Biol* 329 (2003) 371-380.
[24] D. Liang, Fundamentals of X-ray crystallography, *Science Press/Alpha Science International Ltd.*, Beijing ; Oxford, 2011.
[25] G. Rhodes, Crystallography made crystal clear : a guide for users of macromolecular models, *Elsevier/Academic Press*, Amsterdam ; Boston, 2006.
[26] J. Cavanagh, Protein NMR spectroscopy : principles and practice, *Academic Press*, Amsterdam ; Boston, 2007.
[27] V. Tugarinov, W.Y. Choy, V.Y. Orekhov, L.E. Kay, *Proc Natl Acad Sci U S A* 102 (2005) 622-627.
[28] P. Hemmer, *Science* 339 (2013) 529-530.
[29] S.K. Misra, J. Freed, Multifrequency Electron Paramagnetic Resonance, *Wiley-VCH*, Berlin, 2011.
[30] H.C. Li, P.G. Fajer, *Biochemistry* 37 (1998) 6628-6635.
[31] T. Arata, T. Aihara, K. Ueda, M. Nakamura, S. Ueki, *Adv Exp Med Biol* 592 (2007) 125-135.
[32] W. Lehman, A. Galinska-Rakoczy, V. Hatch, L.S. Tobacman, R. Craig, *J Mol Biol* 388 (2009) 673-681.
[33] D. Kowlessur, L.S. Tobacman, *J Biol Chem* 285 (2010) 2686-2694.
[34] W.T. Heller, N.L. Finley, W.J. Dong, P. Timmins, H.C. Cheung, P.R. Rosevear, J. Trewhella, *Biochemistry* 42 (2003) 7790-7800.
[35] J.R. Pearlstone, M. Chandra, M.M. Sorenson, L.B. Smillie, *J Biol Chem* 275 (2000) 35106-35115.
[36] L. Smith, C. Tainter, M. Regnier, D.A. Martyn, *Biophys J* 96 (2009) 3692-3702.
[37] N.M. Kad, S. Kim, D.M. Warshaw, P. VanBuren, J.E. Baker, *Proc Natl Acad Sci U S A* 102 (2005) 16990-16995.
[38] J.P. Jin, S.M. Chong, *Arch Biochem Biophys* 500 (2010) 144-150.
[39] Y. Au, *Cell Mol Life Sci* 61 (2004) 3016-3033.
[40] A.M. Gordon, E. Homsher, M. Regnier, *Physiol Rev* 80 (2000) 853-924.

[41] W. Lehman, R. Craig, *J Muscle Res Cell Motil* 25 (2004) 455-466.
[42] H.L. Sweeney, R.M. Brito, P.R. Rosevear, J.A. Putkey, *Proc Natl Acad Sci U S A* 87 (1990) 9538-9542.
[43] D. Chin, A.R. Means, *Trends Cell Biol* 10 (2000) 322-328.
[44] N. Finley, A. Dvoretsky, P.R. Rosevear, *J Mol Cell Cardiol* 32 (2000) 1439-1446.
[45] G.A. Krudy, R.M. Brito, J.A. Putkey, P.R. Rosevear, *Biochemistry* 31 (1992) 1595-1602.
[46] V.L. Filatov, A.G. Katrukha, T.V. Bulargina, N.B. Gusev, *Biochemistry (Mosc)* 64 (1999) 969-985.
[47] G. Trigo-Gonzalez, G. Awang, K. Racher, K. Neden, T. Borgford, *Biochemistry* 32 (1993) 9826-9831.
[48] H. Kawasaki, R.H. Kretsinger, *Protein Profile* 1 (1994) 343-517.
[49] W. Liu, D.G. Dotson, X. Lin, J.J. Mullen, 3rd, M.L. Gonzalez-Garay, Q. Lu, J.A. Putkey, *FEBS Lett* 347 (1994) 152-156.
[50] M.X. Li, S.M. Gagne, L. Spyracopoulos, C.P. Kloks, G. Audette, M. Chandra, R.J. Solaro, L.B. Smillie, B.D. Sykes, *Biochemistry* 36 (1997) 12519-12525.
[51] S.K. Sia, M.X. Li, L. Spyracopoulos, S.M. Gagne, W. Liu, J.A. Putkey, B.D. Sykes, *J Biol Chem* 272 (1997) 18216-18221.
[52] M.X. Li, L. Spyracopoulos, B.D. Sykes, *Biochemistry* 38 (1999) 8289-8298.
[53] W.J. Dong, J. Xing, M. Villain, M. Hellinger, J.M. Robinson, M. Chandra, R.J. Solaro, P.K. Umeda, H.C. Cheung, *J Biol Chem* 274 (1999) 31382-31390.
[54] S. Ueki, M. Nakamura, T. Komori, T. Arata, *Biochemistry* 44 (2005) 411-416.
[55] G. De Nicola, C. Burkart, F. Qiu, B. Agianian, S. Labeit, S. Martin, B. Bullard, A. Pastore, *Structure* 15 (2007) 813-824.
[56] S.R. Martin, G. Avella, M. Adrover, G.F. de Nicola, B. Bullard, A. Pastore, *Biochemistry* 50 (2011) 1839-1847.
[57] G.M. Gasmi-Seabrook, J.W. Howarth, N. Finley, E. Abusamhadneh, V. Gaponenko, R.M. Brito, R.J. Solaro, P.R. Rosevear, *Biochemistry* 38 (1999) 8313-8322.
[58] W.J. Dong, J. Xing, M. Chandra, J. Solaro, H.C. Cheung, *Proteins* 41 (2000) 438-447.
[59] J.W. Howarth, J. Meller, R.J. Solaro, J. Trewhella, P.R. Rosevear, *J Mol Biol* 373 (2007) 706-722.
[60] G.M. Bou-Assaf, J.E. Chamoun, M.R. Emmett, P.G. Fajer, A.G. Marshall, *Int J Mass Spectrom* 302 (2011) 116-124.
[61] W.J. Dong, J. Xing, J.M. Robinson, H.C. Cheung, *J Mol Biol* 314 (2001) 51-61.
[62] W.J. Dong, J.M. Robinson, S. Stagg, J. Xing, H.C. Cheung, *J Biol Chem* 278 (2003) 8686-8692.
[63] W.J. Dong, J. An, J. Xing, H.C. Cheung, *Arch Biochem Biophys* 456 (2006) 135-142.
[64] R.M. Hoffman, T.M. Blumenschein, B.D. Sykes, *J Mol Biol* 361 (2006) 625-633.
[65] R.T. McKay, B.P. Tripet, R.S. Hodges, B.D. Sykes, *J Biol Chem* 272 (1997) 28494-28500.
[66] T.M. Blumenschein, D.B. Stone, R.J. Fletterick, R.A. Mendelson, B.D. Sykes, *Biophys J* 90 (2006) 2436-2444.
[67] J. Xing, M. Chinnaraj, Z. Zhang, H.C. Cheung, W.J. Dong, *Biochemistry* 47 (2008) 13383-13393.
[68] R.T. McKay, L.F. Saltibus, M.X. Li, B.D. Sykes, *Biochemistry* 39 (2000) 12731-12738.

[69] V. Gaponenko, E. Abusamhadneh, M.B. Abbott, N. Finley, G. Gasmi-Seabrook, R.J. Solaro, M. Rance, P.R. Rosevear, *J Biol Chem* 274 (1999) 16681-16684.
[70] N. Finley, M.B. Abbott, E. Abusamhadneh, V. Gaponenko, W. Dong, G. Gasmi-Seabrook, J.W. Howarth, M. Rance, R.J. Solaro, H.C. Cheung, P.R. Rosevear, *FEBS Lett* 453 (1999) 107-112.
[71] M.B. Abbott, W.J. Dong, A. Dvoretsky, B. DaGue, R.M. Caprioli, H.C. Cheung, P.R. Rosevear, *Biochemistry* 40 (2001) 5992-6001.
[72] O.K. Baryshnikova, M.X. Li, B.D. Sykes, *J Mol Biol* 375 (2008) 735-751.
[73] S. Sadayappan, N. Finley, J.W. Howarth, H. Osinska, R. Klevitsky, J.N. Lorenz, P.R. Rosevear, J. Robbins, *FASEB J* 22 (2008) 1246-1257.
[74] R.J. Solaro, P. Rosevear, T. Kobayashi, *Biochem Biophys Res Commun* 369 (2008) 82-87.
[75] T. Kobayashi, W.J. Dong, E.M. Burkart, H.C. Cheung, R.J. Solaro, *Biochemistry* 43 (2004) 5996-6004.
[76] S. Sakthivel, N.L. Finley, P.R. Rosevear, J.N. Lorenz, J. Gulick, S. Kim, P. VanBuren, L.A. Martin, J. Robbins, *J Biol Chem* 280 (2005) 703-714.
[77] B. You, G. Yan, Z. Zhang, L. Yan, J. Li, Q. Ge, J.P. Jin, J. Sun, *Biochem J* 418 (2009) 93-101.
[78] Y. Ouyang, R. Mamidi, J.J. Jayasundar, M. Chandra, W.J. Dong, *J Mol Biol* 400 (2010) 1036-1045.
[79] B.R. Nixon, A. Thawornkaiwong, J. Jin, E.A. Brundage, S.C. Little, J.P. Davis, R.J. Solaro, B.J. Biesiadecki, *J Biol Chem* 287 (2012) 19136-19147.
[80] S.M. Chong, J.P. Jin, *J Mol Evol* 68 (2009) 448-460.
[81] B. Wei, J.P. Jin, *Arch Biochem Biophys* 505 (2011) 144-154.
[82] J.P. Jin, Z. Zhang, J.A. Bautista, *Crit Rev Eukaryot Gene Expr* 18 (2008) 93-124.
[83] R. Mamidi, S.L. Mallampalli, D.F. Wieczorek, M. Chandra, *J Physiol* 591 (2013) 1217-1234.
[84] R. Mamidi, J.J. Michael, M. Muthuchamy, M. Chandra, *FASEB J* 27 (2013) 3848-3859.
[85] M.P. Sumandea, W.G. Pyle, T. Kobayashi, P.P. de Tombe, R.J. Solaro, *J Biol Chem* 278 (2003) 35135-35144.
[86] T. Kobayashi, L. Jin, P.P. de Tombe, *Pflugers Arch* 457 (2008) 37-46.
[87] A. Dvoretsky, E.M. Abusamhadneh, J.W. Howarth, P.R. Rosevear, *J Biol Chem* 277 (2002) 38565-38570.
[88] G.A. Olah, S.E. Rokop, C.L. Wang, S.L. Blechner, J. Trewhella, *Biochemistry* 33 (1994) 8233-8239.
[89] D.B. Stone, P.A. Timmins, D.K. Schneider, I. Krylova, C.H. Ramos, F.C. Reinach, R.A. Mendelson, *J Mol Biol* 281 (1998) 689-704.
[90] W.A. King, D.B. Stone, P.A. Timmins, T. Narayanan, A.A. von Brasch, R.A. Mendelson, P.M. Curmi, *J Mol Biol* 345 (2005) 797-815.
[91] Q. Kleerekoper, J.W. Howarth, X. Guo, R.J. Solaro, P.R. Rosevear, *Biochemistry* 34 (1995) 13343-13352.
[92] M.B. Abbott, A. Dvoretsky, V. Gaponenko, P.R. Rosevear, *FEBS Lett* 469 (2000) 168-172.
[93] W.J. Dong, J.M. Robinson, J. Xing, P.K. Umeda, H.C. Cheung, *Protein Sci* 9 (2000) 280-289.
[94] L. Schrödinger, The PyMOL Molecular Graphics System, Version 1.1r1, 2008.

[95] D.G. Ward, S.M. Brewer, C.E. Gallon, Y. Gao, B.A. Levine, I.P. Trayer, *Biochemistry* 43 (2004) 5772-5781.
[96] D.G. Ward, S.M. Brewer, M.J. Calvert, C.E. Gallon, Y. Gao, I.P. Trayer, *Biochemistry* 43 (2004) 4020-4027.
[97] W.T. Heller, E. Abusamhadneh, N. Finley, P.R. Rosevear, J. Trewhella, *Biochemistry* 41 (2002) 15654-15663.
[98] N.J. Greenfield, Y.J. Huang, G.V. Swapna, A. Bhattacharya, B. Rapp, A. Singh, G.T. Montelione, S.E. Hitchcock-DeGregori, *J Mol Biol* 364 (2006) 80-96.
[99] S.E. Hitchcock-DeGregori, Y. An, *J Biol Chem* 271 (1996) 3600-3603.
[100] F. Matsumoto, K. Makino, K. Maeda, H. Patzelt, Y. Maeda, S. Fujiwara, *J Mol Biol* 342 (2004) 1209-1221.
[101] A. Galinska-Rakoczy, P. Engel, C. Xu, H. Jung, R. Craig, L.S. Tobacman, W. Lehman, *J Mol Biol* 379 (2008) 929-935.
[102] J. Xing, J.J. Jayasundar, Y. Ouyang, W.J. Dong, *J Biol Chem* 284 (2009) 16432-16441.
[103] Z. Zhou, D. Rieck, K.L. Li, Y. Ouyang, W.J. Dong, *Arch Biochem Biophys* (2013).
[104] M. Nakamura, S. Ueki, H. Hara, T. Arata, *J Mol Biol* 348 (2005) 127-137.
[105] T. Burgoyne, F. Muhamad, P.K. Luther, *Cardiovasc Res* 77 (2008) 707-712.
[106] A. Narita, T. Yasunaga, T. Ishikawa, K. Mayanagi, T. Wakabayashi, *J Mol Biol* 308 (2001) 241-261.
[107] Y.B. Sun, M. Irving, *J Mol Cell Cardiol* 48 (2010) 859-865.
[108] X.E. Li, W. Lehman, S. Fischer, *J Struct Biol* 170 (2010) 313-318.
[109] R.F. Rayes, T. Kalai, K. Hideg, M.A. Geeves, P.G. Fajer, *PLoS One* 6 (2011) e21277.
[110] R.W. Kensler, *Biophys J* 82 (2002) 1497-1508.
[111] H.A. Al-Khayat, R.W. Kensler, J.M. Squire, S.B. Marston, E.P. Morris, *Proc Natl Acad Sci U S A* 110 (2013) 318-323.
[112] M. Suzuki, S. Ishiwata, *Biophys J* 101 (2011) 2740-2748.
[113] R. Craig, W. Lehman, *J Mol Biol* 311 (2001) 1027-1036.
[114] W.A. Mudalige, T.C. Tao, S.S. Lehrer, *J Mol Biol* 389 (2009) 575-583.
[115] X.E. Li, L.S. Tobacman, J.Y. Mun, R. Craig, S. Fischer, W. Lehman, *Biophys J* 100 (2011) 1005-1013.
[116] S.S. Lehrer, *J Muscle Res Cell Motil* 32 (2010) 203-208.
[117] G.P. Farman, D. Gore, E. Allen, K. Schoenfelt, T.C. Irving, P.P. de Tombe, *Am J Physiol Heart Circ Physiol* 300 (2011) H2155-2160.
[118] P.P. de Tombe, R.D. Mateja, K. Tachampa, Y. Ait Mou, G.P. Farman, T.C. Irving, *J Mol Cell Cardiol* 48 (2010) 851-858.
[119] S. Wu, J. Liu, M.C. Reedy, R.J. Perz-Edwards, R.T. Tregear, H. Winkler, C. Franzini-Armstrong, H. Sasaki, C. Lucaveche, Y.E. Goldman, M.K. Reedy, K.A. Taylor, *PLoS One* 7 (2012) e39422.
[120] R.L. Moss, M. Razumova, D.P. Fitzsimons, *Circ Res* 94 (2004) 1290-1300.
[121] J.D. Hannon, D.A. Martyn, A.M. Gordon, *Circ Res* 71 (1992) 984-991.
[122] D.A. Martyn, M. Regnier, D. Xu, A.M. Gordon, *Biophys J* 80 (2001) 360-370.
[123] M.X. Li, S.M. Gagne, S. Tsuda, C.M. Kay, L.B. Smillie, B.D. Sykes, *Biochemistry* 34 (1995) 8330-8340.
[124] X. Lin, G.A. Krudy, J. Howarth, R.M. Brito, P.R. Rosevear, J.A. Putkey, *Biochemistry* 33 (1994) 14434-14442.

[125] L. Spyracopoulos, M.X. Li, S.K. Sia, S.M. Gagne, M. Chandra, R.J. Solaro, B.D. Sykes, *Biochemistry* 36 (1997) 12138-12146.
[126] N.M. Cordina, C.K. Liew, D.A. Gell, P.G. Fajer, J.P. Mackay, L.J. Brown, *Biochemistry* (2013).
[127] K. Paakkonen, A. Annila, T. Sorsa, P. Pollesello, C. Tilgmann, I. Kilpelainen, P. Karisola, I. Ulmanen, T. Drakenberg, *J Biol Chem* 273 (1998) 15633-15638.
[128] K. Paakkonen, T. Sorsa, T. Drakenberg, P. Pollesello, C. Tilgmann, P. Permi, S. Heikkinen, I. Kilpelainen, A. Annila, *Eur J Biochem* 267 (2000) 6665-6672.
[129] J.M. Robinson, H.C. Cheung, W. Dong, *Biophys J* 95 (2008) 4772-4789.
[130] D.C. Rieck, K.L. Li, Y. Ouyang, R.J. Solaro, W.J. Dong, *Arch Biochem Biophys* 537 (2013) 198-209.
[131] A. Galinska, V. Hatch, R. Craig, A.M. Murphy, J.E. Van Eyk, C.L. Wang, W. Lehman, D.B. Foster, *Circ Res* 106 (2010) 705-711.
[132] W.J. Dong, C.K. Wang, A.M. Gordon, S.S. Rosenfeld, H.C. Cheung, *J Biol Chem* 272 (1997) 19229-19235.
[133] W.J. Dong, J.J. Jayasundar, J. An, J. Xing, H.C. Cheung, *Biochemistry* 46 (2007) 9752-9761.
[134] R. Stehle, J. Solzin, B. Iorga, C. Poggesi, *Pflugers Arch* 458 (2009) 337-357.
[135] K.L. Kreutziger, N. Piroddi, J.T. McMichael, C. Tesi, C. Poggesi, M. Regnier, *J Mol Cell Cardiol* 50 (2011) 165-174.
[136] D.R. Swartz, Z. Yang, A. Sen, S.B. Tikunova, J.P. Davis, *J Mol Biol* 361 (2006) 420-435.
[137] M.G. Bell, E.B. Lankford, G.E. Gonye, G.C. Ellis-Davies, D.A. Martyn, M. Regnier, R.J. Barsotti, *Biophys J* 90 (2006) 531-543.
[138] T.E. Gillis, D.A. Martyn, A.J. Rivera, M. Regnier, *J Physiol* 580 (2007) 561-576.
[139] M. Regnier, A.J. Rivera, C.K. Wang, M.A. Bates, P.B. Chase, A.M. Gordon, *J Physiol* 540 (2002) 485-497.
[140] V.L. Korman, V. Hatch, K.Y. Dixon, R. Craig, W. Lehman, L.S. Tobacman, *J Biol Chem* 275 (2000) 22470-22478.
[141] T.I. Bekyarova, M.C. Reedy, B.A. Baumann, R.T. Tregear, A. Ward, U. Krzic, K.M. Prince, R.J. Perz-Edwards, M. Reconditi, D. Gore, T.C. Irving, M.K. Reedy, *Proc Natl Acad Sci U S A* 105 (2008) 10372-10377.
[142] W.J. Dong, M. Chandra, J. Xing, R.J. Solaro, H.C. Cheung, *Biochemistry* 36 (1997) 6745-6753.